

# DRAFT COPY

Progress Report

Nov 1980

FLUIDIC MUD PULSE TELEMETRY  
TECHNOLOGY INVESTIGATIONS FOR  
MEASUREMENT WHILE DRILLING  
APPLICATIONS

Prepared by:

Allen B. Holmes  
U.S. Harry Diamond Laboratories  
2800 Powder Mill Road  
Adelphi, MD 20783  
202/394-3080

### Acknowledgements

The authors wish to express their appreciation to John Gregory of the U.S. Geological Survey, Oil and Gas Conservation Division for his support.

We would like also to express our appreciation to the Drilling Research personnel under the direction of Alan Black who conducted over 80 hours of testing after normal working hours.

## CONTENTS

SUMMARY

INTRODUCTION

VORTEX VALVES

FLUID AMPLIFIERS

PULSER CIRCUIT A

PULSER CIRCUIT B

MULTI-STAGE CIRCUITS

TEST HARDWARE

TEST PROGRAM

RESULTS

DISCUSSION OF RESULTS

CONCLUSIONS

## ILLUSTRATIONS

Figure 1. Schematic view showing the relationship between elements in a mud pulse telemetry system.

Figure 2. Illustration of (a) vortex valve end (b) fluid amplifier components.

Figure 3. Illustration of 2-stage fluidic pulser circuits.

Figure 4. Artist's drawing showing (a) 4-stage A-type fluidic mud pulser circuit (b) 3-stage B-type valve assembly.

Figure 5. Fluidic test hardware.

Figure 6. Photographs showing (a) A-type circuit test hardware, (b) B-type circuit test hardware.

Figure 6. Photograph showing (a) A-type circuit test hardware, (b) B-type circuit test hardware.

Figure 7. Photograph showing A-type circuit components.

Figure 8. Photographs showing (a) test circuit A (b) test circuit A prior to insertion into test chamber.

Figure 9. Photographs showing (a) test hardware being installed in chamber (b) test hardware being removed from chamber.

Figure 10. Test setup.

Figure 11. Calculated flow areas from test data.

Figure 12. Test circuit A operating at 40 gpm per stage at 2 Hz.

Figure 13. Circuit A operating at 114 gpm per stage for one second at 2 Hz.

Figure 14. Circuit B operating at 130 gpm per stage for 10 seconds at 1 Hz.

Figure 15. Circuit B operating at 130 gpm per stage at 8 Hz for (a) 10 seconds (b) 1 second, (c) 0.2 seconds.

Figure 16. Calculated (a) signal pressures (b) pressure drop across given areas for specified circulating flow conditions.

## SUMMARY

This report describes the progress, status, and results of on-going Fluidic Research Mud Pulse Technology Investigations at the U.S. Harry Diamond Laboratories. The work reported is sponsored by the U.S. Geological Survey Research and Development Program for the Outer Continental Shelf.

The program focuses on the development and evaluation of advanced fluidic approaches to mud pulse valve design. The goal is to develop the technology required to produce a highly reliable, high capacity (200 - 800 gpm), fast-acting (5 to 25 pulses per second) valve for transmitting information on bottom hole conditions affecting safety while drilling.

This report contains a description of two unique valve design approaches which have been demonstrated in this program. The concepts center upon the use of multiple stage fluidic vortex valving techniques in place of conventional moving part type valving technologies. Experimental results from flow tests on a short line are used to demonstrate operation of experimental devices at flow rates equal to 130 gpm per stage and pulse rates up to 8 pulses per second. Analysis procedures are described for using the test data to predict functional capabilities on a long line including effects of hole depths, drill bit area, viscosity, and pulse rate on operating pressure drop, signal amplitude and attenuation.

5

## INTRODUCTION

In a mud pulsing system, a valve located near the bit (figure 1) is used to restrict and release the circulating fluid in the drill string. Each time the valve is partially closed and reopened, a change in flow rate occurs which in turn converts a portion of the kinetic energy (velocity) of the incoming fluid to potential energy (pressure). The result is a pressure wave which travels up the drill pipe through the mud at the speed of sound (approximately 4700 ft/sec). A sequence of waves represent coded information from bore hole instruments. The waves are detected at the surface with a pressure transducer, decoded, and displayed to the driller. In a fluidic mud pulse telemetry system, the pressure waves are produced by the restrictive action of a vortex. The vortex flow action determines the effective port area in the same manner as the movement of a poppet or a similar device changes the resistance of a valve outlet port.

## FLUIDIC MUD PULSERS

A fluidic mud pulser is essentially a variable flow restrictor which provides the required change in flow resistance by means of a constrained vortex. The pulser exhibits its maximum resistance to flow (minimum effective port area) when a vortex is generated. The valve produces its minimum resistance to flow (maximum effective port area) when no vortex is present. The transition between the vortex and non-vortex operating mode is produced in response to electrical commands. The physical features of the components used in a fluidic mud pulser circuit are illustrated in figure 2. Two valving circuits are shown in figure 3.

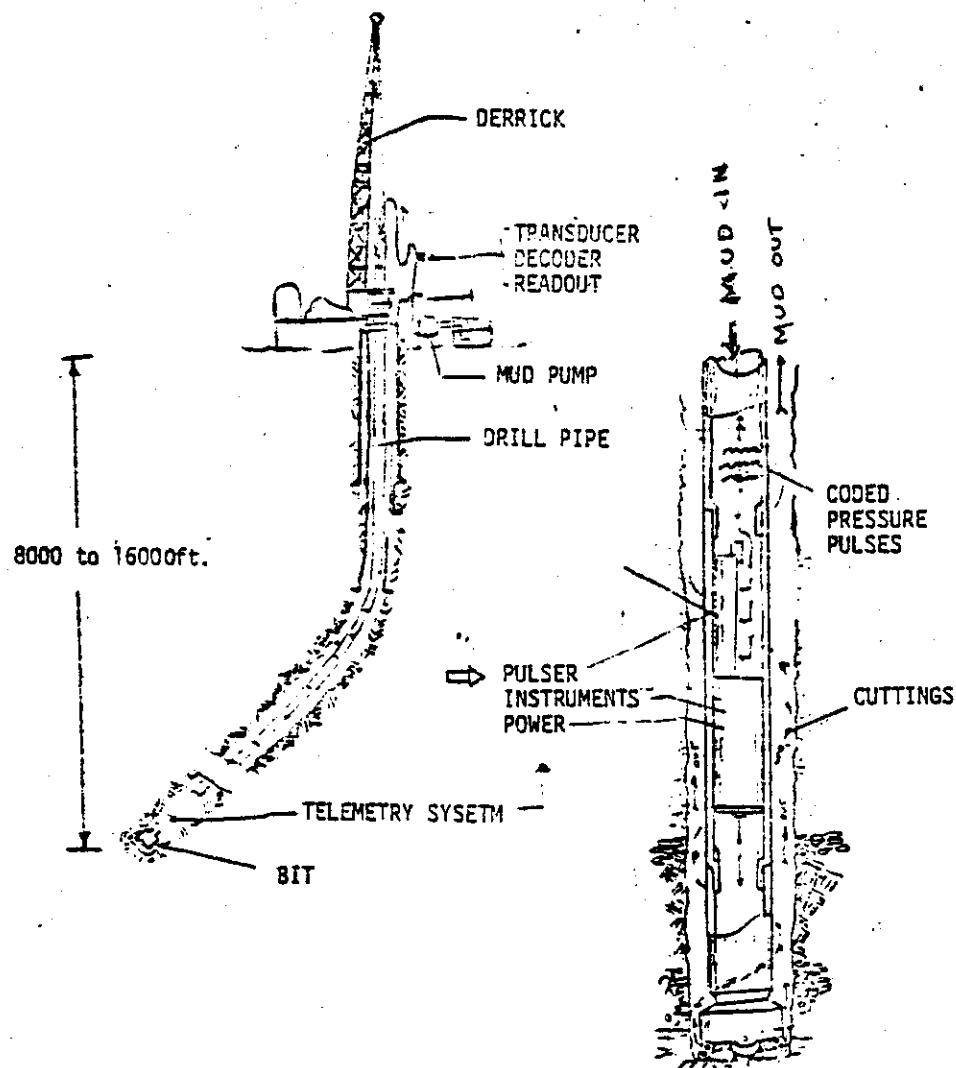


Figure 1. Mud Pulse Telemetry in a circulating system.

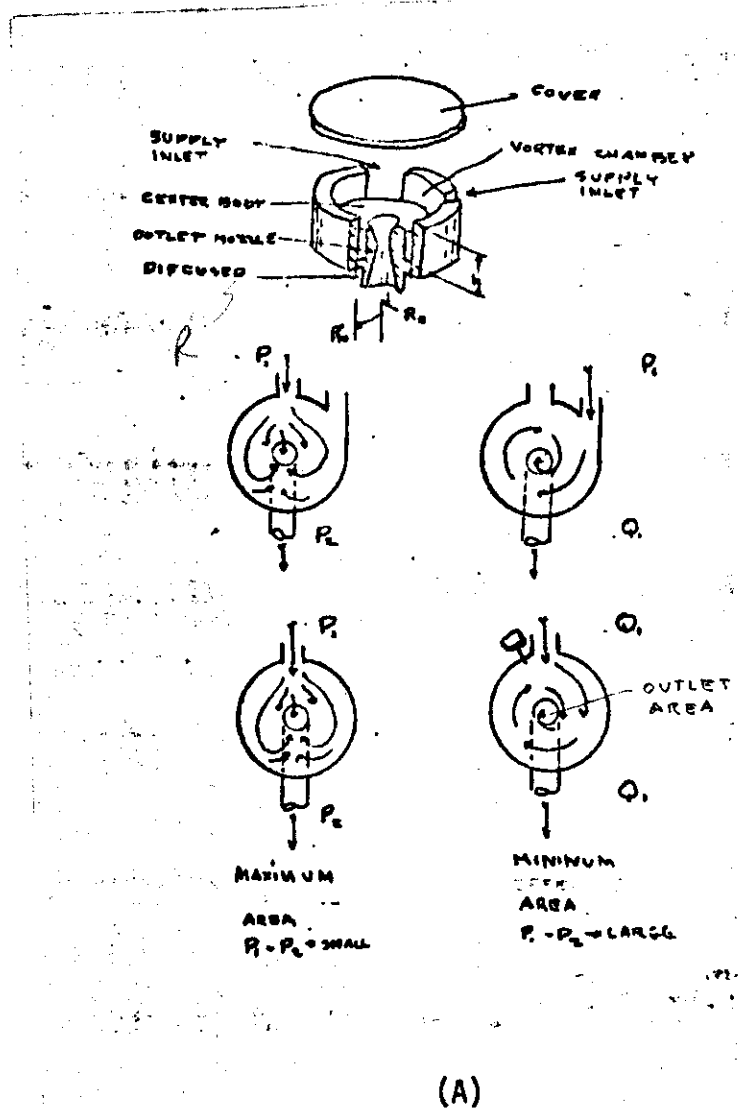
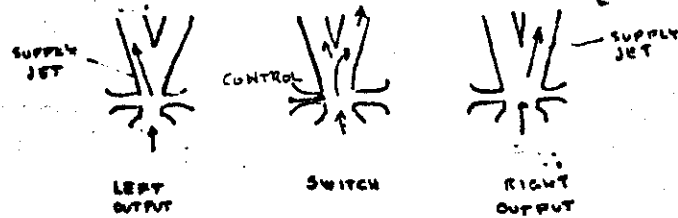
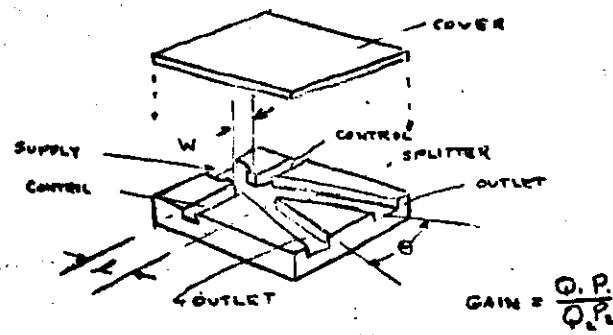


Figure 2a Vortex valve construction and operation





(B)

Figure 2b Fluid amplifier assembly and operation.

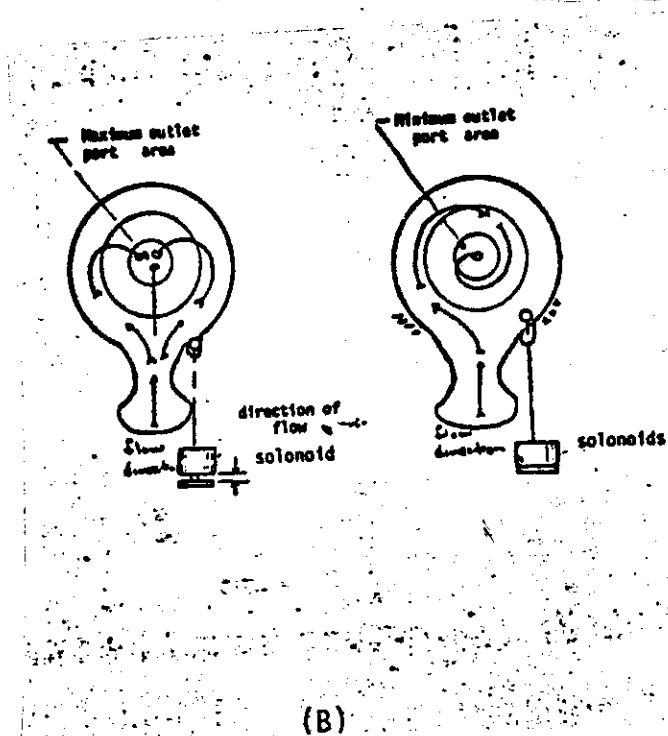
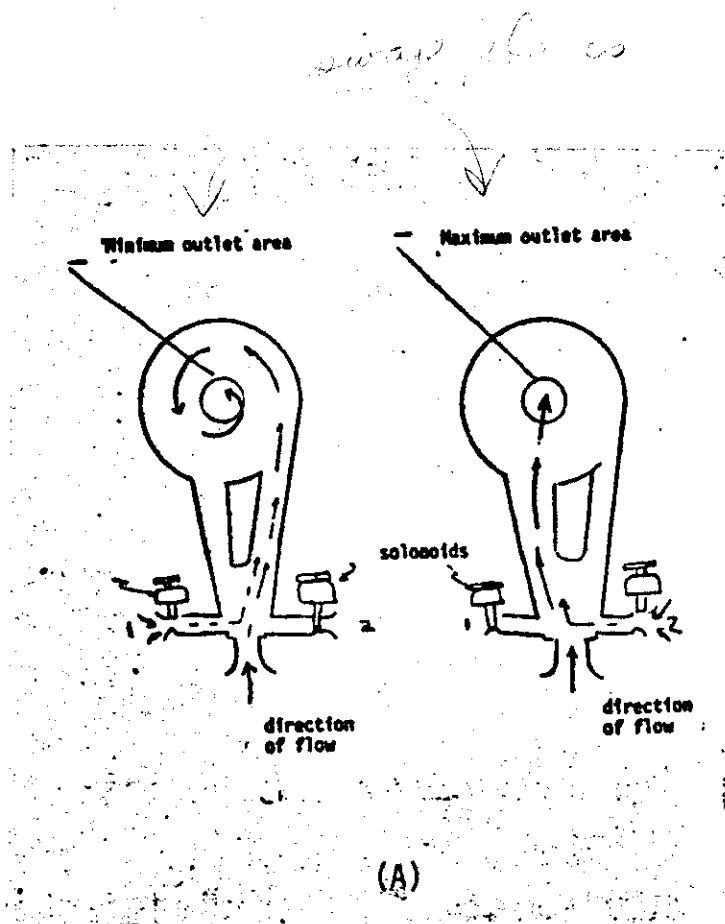


Figure 3 Principle operating features of (A) an A-Type pulser circuit stage, (B) a B-Type circuit stage.

## FLUID AMPLIFIERS

The flow geometry and operation of a digital fluid amplifier is illustrated in figure 2b. In a digital fluid amplifier, each side of the supply jet is bounded by a wall downstream of two opposing control nozzles. The Coanda effect--a turbulent jet's property of attaching itself to a surface--causes the flow through these devices to be bistable. This means that a continuous control flow is not required to keep the supply jet directed at any single outlet. Diversion of the supply flow between outlets occurs when pressure is supplied to a control jet and sufficient energy is supplied to separate the supply jet from the wall. Amplification occurs in the sense that the peak flow rate delivered by the control jet is 10 to 100 times less than the supply flow rate.

The gain of an amplifier is the ratio between the supply flow rate and the control flow rate at the switching point. Gain is determined by geometric parameters such as the relative distance between the nozzle walls ( $W$ ), distance to the splitter in terms of ( $W$ ), setback  $w/d$  where ( $d$ ) equals the distance between the walls of the nozzle exhaust plane and the wall divergence angle ( $\theta$ ). Gain is primarily a measurement of how little the supply jet must be deflected before reattachment occurs on the opposite wall.

The response time of an amplifier is a measure of the time required to divert the supply jet between outlets. Response time is dependent upon the geometric parameters described above and also the properties of the supply fluid. A general rule of thumb is that the time required for flow diversion is approximately equal to 3 times the transport time between the nozzle and splitter regardless of the magnitude of the control signal.

## VORTEX VALVES

Figure 2a shows the internal shape of a vortex valve. The valve contains one or more inlet ports, a vortex chamber, a centerbody and an outlet nozzle-diffuser assembly. The outlet nozzle exhibits two effective flow areas which are dependent upon the direction of flow in the vortex chamber. A valve exhibits its minimum resistance when the flow passes directly to the outlet. A valve exhibits maximum resistance to flow when a vortex is present. The action of the vortex produces a large pressure drop across the valve due to the centrifugal force exerted by the rotating fluid. The pressure drop and flow rate are equated to an effective flow area.

The ratio between the maximum and minimum flow area measured under conditions of constant pressure or flow rate is used to define turn-down. Turn-down is a measure of valving effectiveness. The geometric parameters which principally influence turn-down include normalized radius  $r_o/r_e$  where  $r_o$  is the chamber radius,  $r_e$  is the exhaust nozzle radius and  $(h)$  is chamber depth. Other parameters which influence turn-down are  $(W)$  the width of the inlet and the design of the center body and outlet nozzle/diffuser contours.

The response time of a vortex valve is equal to the time required to either form or dissipate the vortex. Response time has been shown by various experimenters to be proportional to the volume of the vortex chamber, and inversely proportional to flow rate. The response time of a vortex valve is generally stated at a specified flow rate.

## CIRCUIT A

In figure 3a, Circuit A contains a fluid amplifier and a vortex valve. In the diagram on the left, flow enters the circuit through the amplifier supply port where it forms a jet which is shown attached to the left wall (solid arrows) leading to the radial inlet to a vortex valve. Since the flow passes directly to the outlet without tangential velocity, no vortex is produced, and the valve is considered to be fully open. The only restriction to flow is produced by the frictional pressure drops in the amplifier, the vortex valve, and the effective discharge area of the outlet.

When a flow signal is applied to port 1, the supply flow separates from the wall of the amplifier and attaches (broken arrows) to the wall leading to the tangential inlet to the vortex valve. When this occurs, a tangential velocity component is imparted to the fluid. Since angular momentum must be conserved, the tangential velocity increases as the flow approaches the outlet. The high tangential velocities in the core of the vortex create the effect of restricting the flow, which, in turn, is equated with an effective reduction in outlet port area. The valve can remain in this state when the control signal is removed. The valve is returned to its original state when a control flow is applied to port 2 of the amplifier.

## CIRCUIT B

The principal features and operation of a B-type circuit are illustrated in figure 3b. A B-type circuit contains a vortex valve with a single radial inlet. The circuit is controlled by placing a small physical obstruction in the vortex chamber to destroy symmetry. As the flow (solid arrows) enters circuit B, it passes directly to the outlet when no control signal (i.e., symmetry) is present. Under this condition the outlet exhibits minimum resistance (maximum area), and the valve is considered open. When the symmetry of the inlet flow (broken arrows) is destroyed, in this example by inserting a tab into the flow, the stream bends towards the wall of the chamber and a vortex is formed which restricts the flow. In the vortex mode the valve exhibits its minimum effective flow area and is considered to be shut down. The flow is returned to its maximum when the tab is retracted.

## FUNCTIONAL CHARACTERISTICS

The functional characteristics of circuits A and B that are of principal importance are the effective flow areas in each operating mode, (i.e. turn-down) and response time.

The maximum and minimum flow areas of a circuit are performance parameters that are usually measured in terms of pressure and flow rate. The maximum effective flow area of an A-type circuit is a function of the pressure recovered in the outlet of the amplifier and vortex valve design. In a B-type circuit, the maximum effective flow area is a function of vortex valve design only.

The minimum flow area of an A-type circuit will generally be higher than that of a B-type circuit with a similar outlet nozzle because of the higher tangential velocity at which the flow enters the vortex chamber. Since the effective flow areas of both kinds of circuits depend principally on the state of the vortex, a given circuit exhibits two effective flow areas which are theoretically constant over a wide range of turbulent flow conditions.

The ratio between the maximum and minimum indicated flow rates of a circuit has been defined as turndown. Turn down can also be envisioned as the equivalent to the change in port area which occurs in a mechanical valve when the poppet approaches the seat. In a fluidic circuit the turn down is never infinite because flow is needed to create the vortex action.

The pressure drop across a vortex valve as with any valve increases as the square of the turndown ratio at constant flow. The flow rate or effective flow area through a circuit is proportional to the turn down ratio at a constant pressure.

The response time of a circuit is essentially a measure of the time required for fluid to pass between the control inlet and supply flow outlet of the circuit. Frequency response, the inverse of response time, increases with flow rate and decreases with circuit volume. The frequency response of a fluid amplifier alone is generally considerably higher than that of a vortex valve because of the shorter path length. In a fluidic pulser circuit, frequency response is maximized by keeping the physical volume of the circuit stages small. This is effectively accomplished in a fluidic valve by staging.

## STAGING

Figure 4 illustrates how multi-stage circuits can be implemented for a mud pulse telemetry application. The principal advantages of using a multi-stage circuit rather than a single large circuit are: staging permits the use of optimum radius relationships, improves frequency performance, and because the volume occupied by the flow channels in any individual circuit will be less than that of a single stage device thus permitting faster response. Staging makes use of the virtually unlimited space along the axis of a drill pipe. In figure 4a, four A-type circuits are arranged in parallel. The 4-stage circuit is driven by a pre-amplifier which, in turn, is controlled by two solenoids. The solenoids are used to drive a slider across the outputs of the pre-amp. Each time flow is diverted in the pre-amp, a signal is produced which pressurizes the amplifier controls. The control signals divert the amplifier flow, thus producing simultaneous signals to drive the vortex valve in the desired operating mode.

The circuit described in figure 4b consists of four vortex valves arranged in parallel. The four valves are activated simultaneously when power is applied to one of the two actuator solenoids. Motion of the solenoid plungers is used to drive a push rod which, in turn, moves tabs into and out of the vortex chamber to drive the vortex into the desired operating mode.

Figure 5 contains a conceptual drawing showing how a multi-stage A-type and B-type fluidic mud pulser could be arranged in a drill pipe.

Figures 6 through 9 contain photographs of the test hardware which was used to implement test circuits.



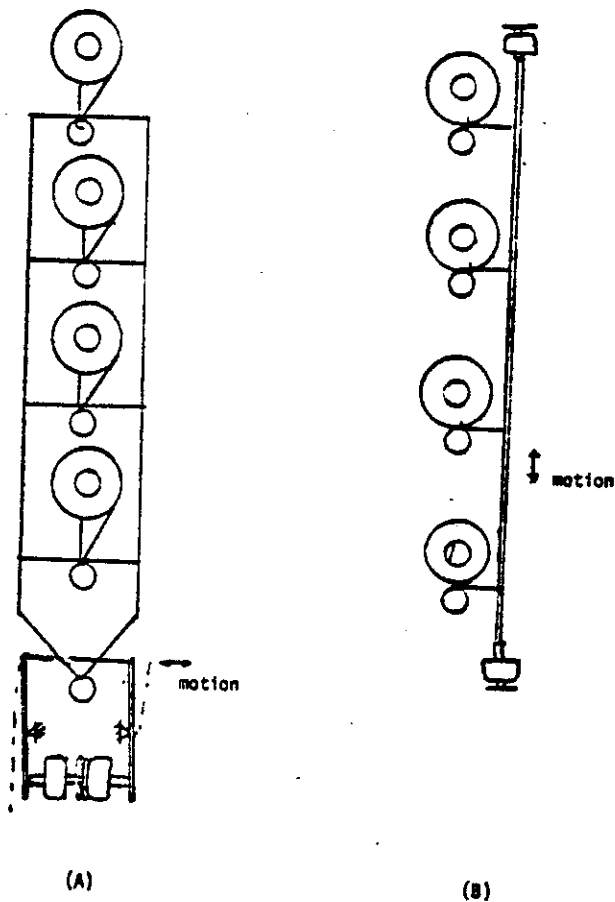


Figure 4 Schematic diagram showing (A) a 4-Stage (A-Type) pulser circuit with a pre-amplifier, (B) a 4-Stage (B-Type) pulser circuit.

# FLUIDIC MUD PULSER

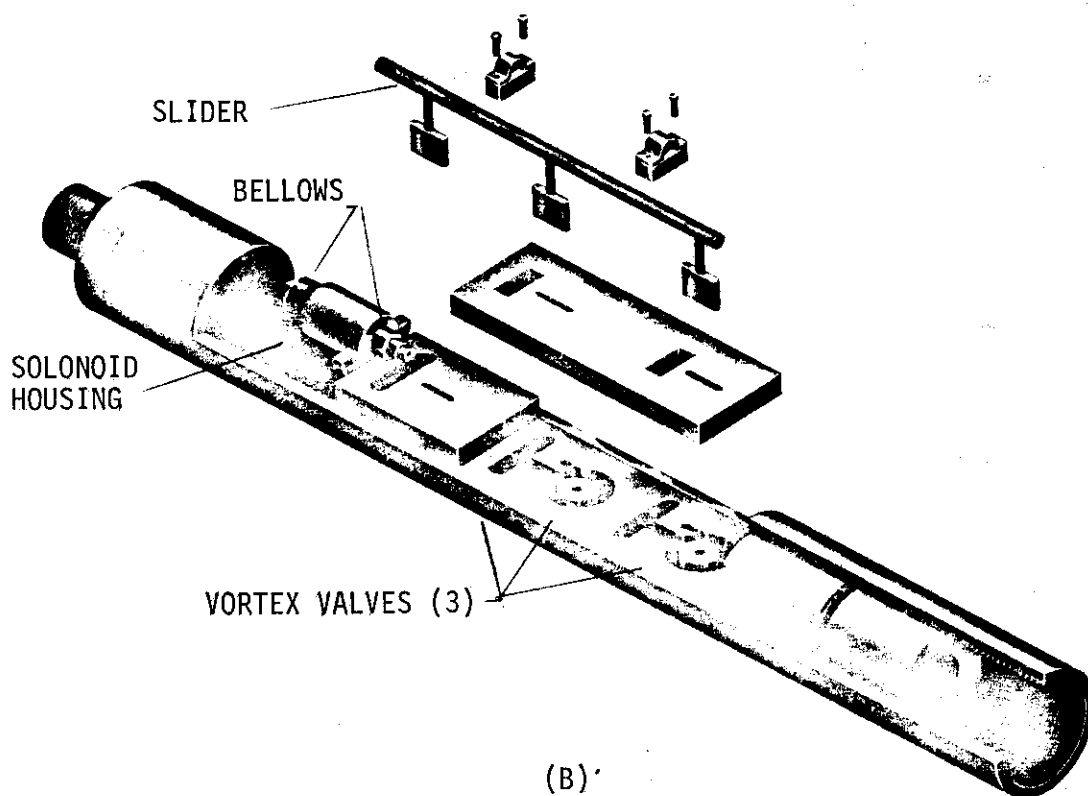
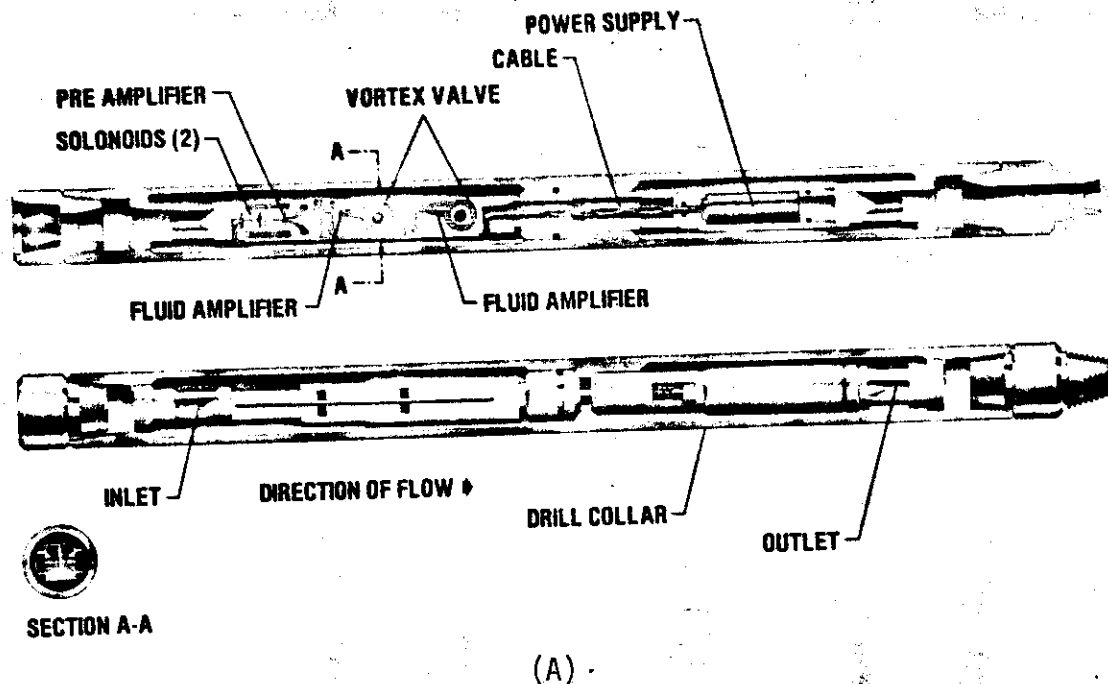


Figure 5 Conceptual drawing illustrating the principle features of two multi-stage fluidic mud pulsers.

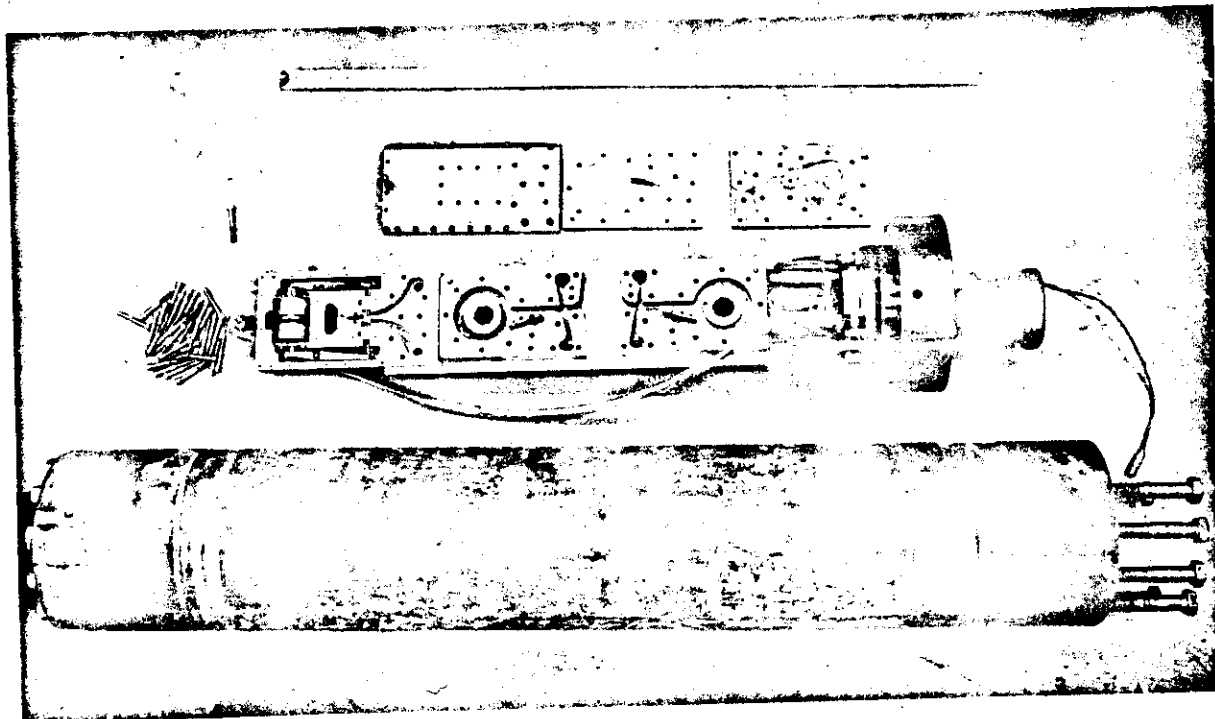


Figure 6 Circuit A test hardware

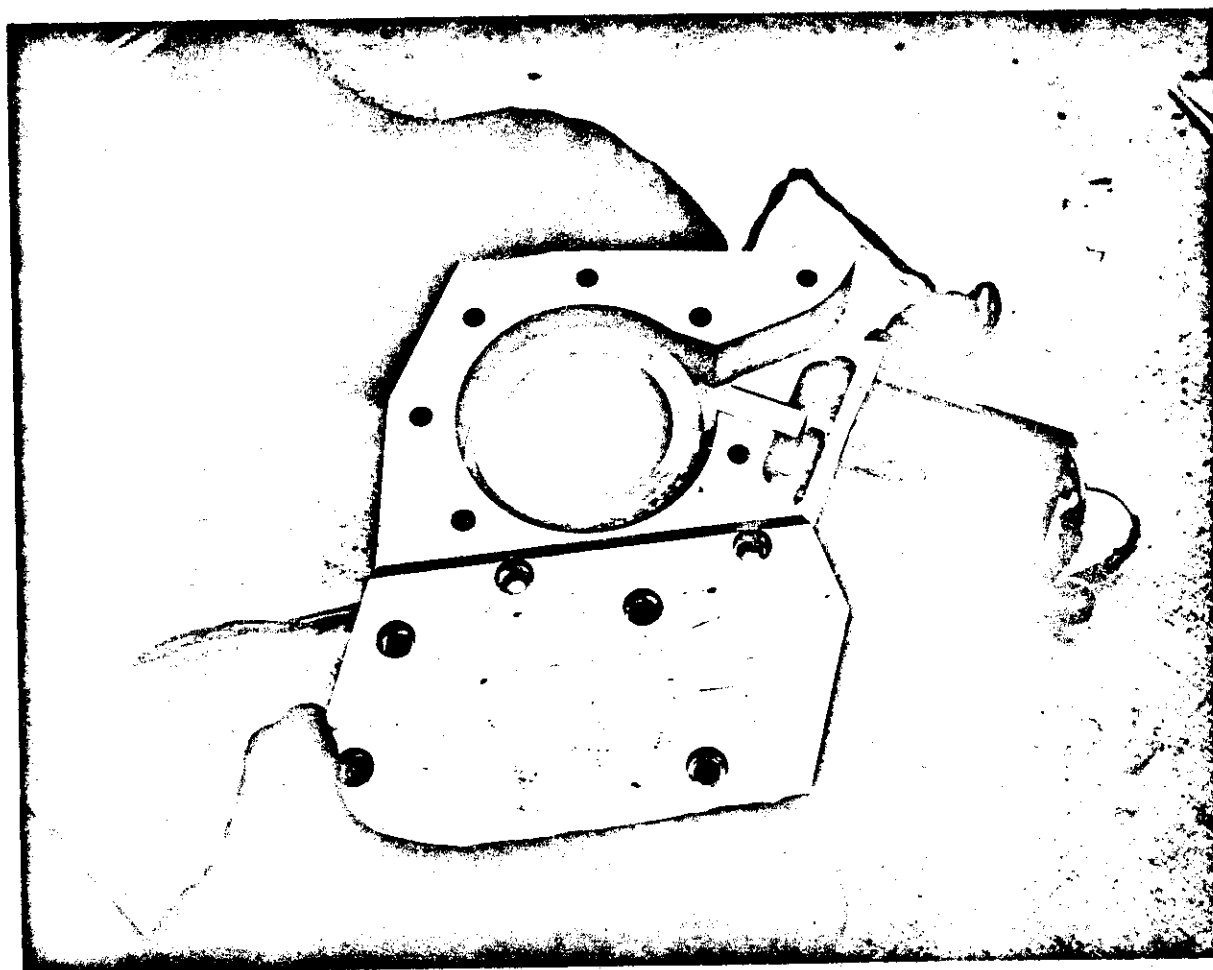


Figure 7 Circuit B test hardware

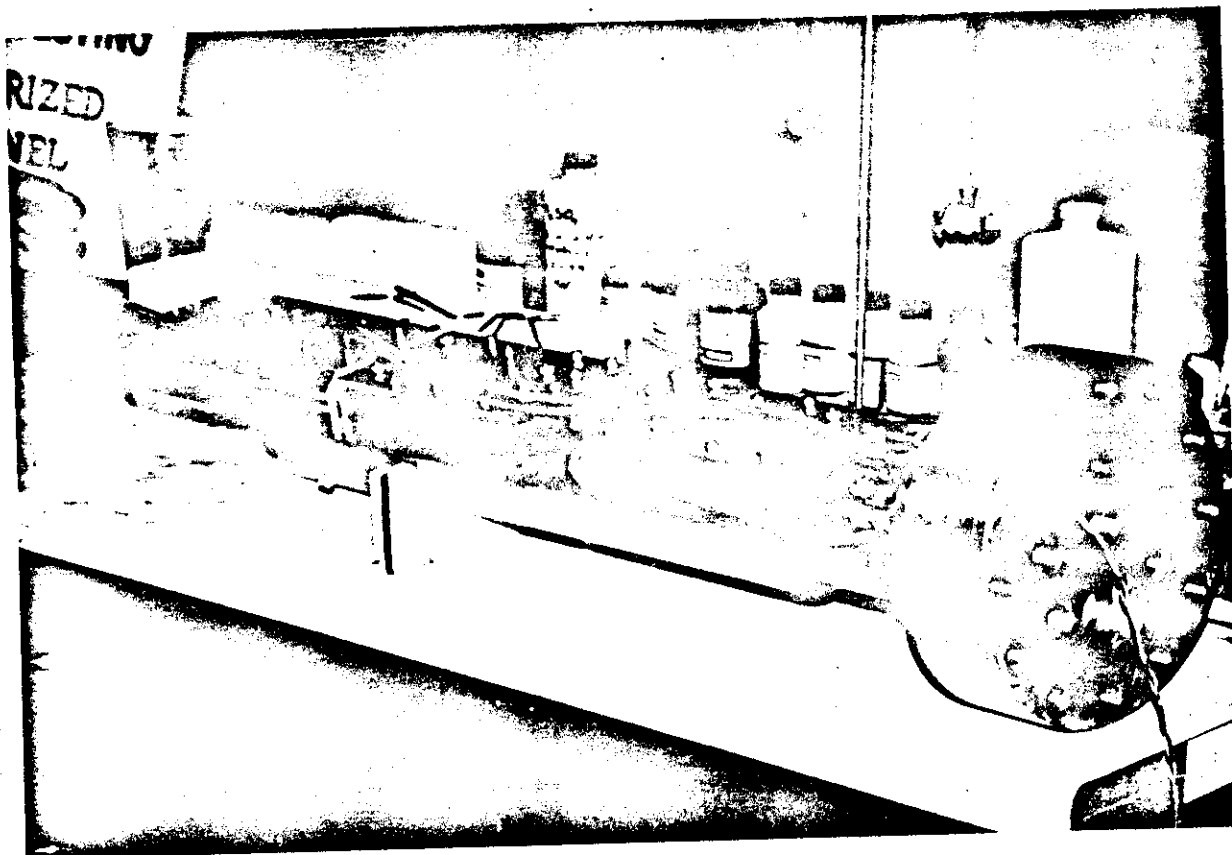


Figure 8 Circuit A test assembly

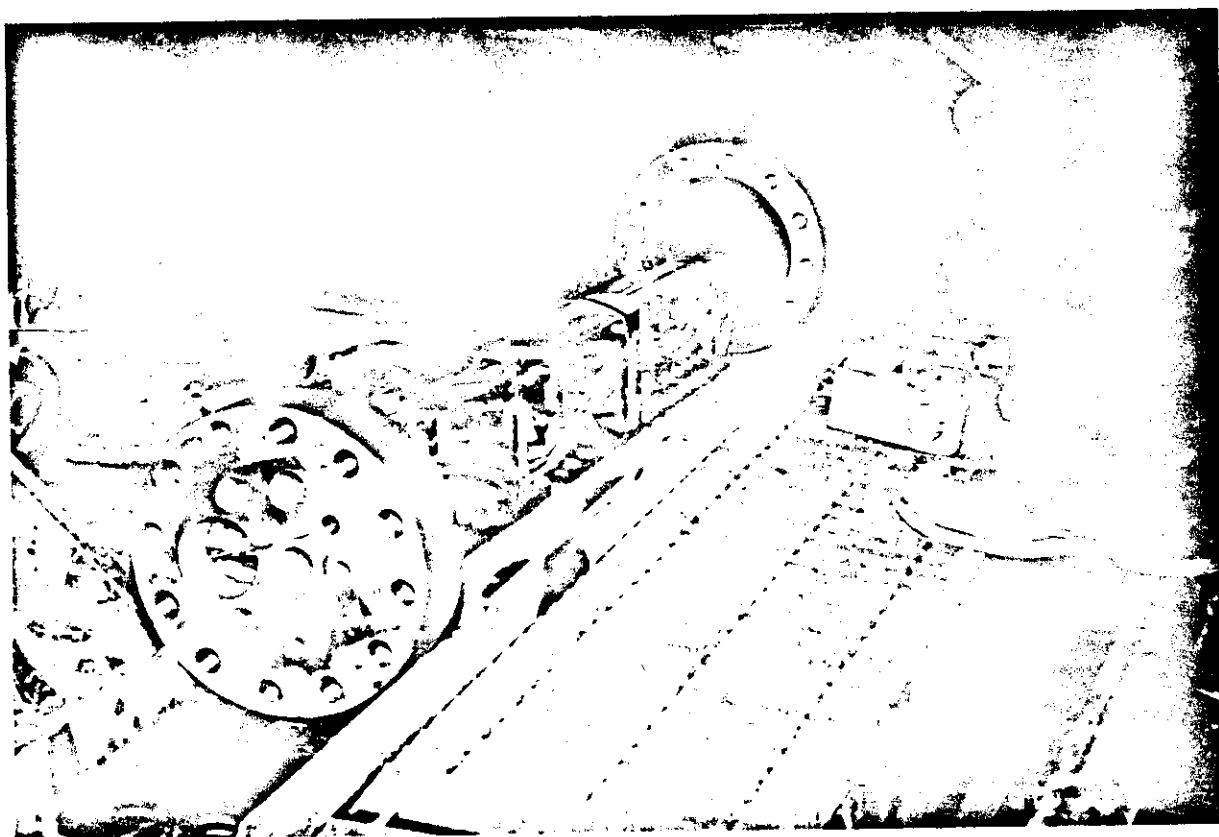


Figure 9 Circuit A test assembly

## TEST HARDWARE

Test hardware was made of steel. Photographs of the test hardware are shown in figure 7. Circuit A was configured as a two-stage valve. Circuit B was fabricated as a single-stage device. The stages were mounted on a manifold containing control and exhaust ducts. The flow was exhausted through a single line connecting the manifold to the mounting flange as shown in the figure 8. The circuits were driven by two solenoids. Electrical energy was supplied via an electrical feed-through connector located on the mounting flange. The maximum frequency response of the solenoid assemblies submerged in water was determined to be 8 Hz. In Circuit A the solenoids were used to drive a slider similar to that shown in figure 3. The slider covered and uncovered the outlet channels in a pre-amp. The Circuit B solenoids were used to inject and retract a tab into and out of the vortex chamber. In each circuit the maximum stroke of the solenoid was approximately 0.150 inches.

Circuit A was operated with several outlet nozzles. The nozzles were of the convergent and convergent-divergent (diffuser) type. Throat diameters of 0.60, 0.70 and 0.875 inches were used. The diffuser exit diameter was equal to 0.875 inches. Circuit B was operated with a 0.7 x 0.875 inch nozzle and the 0.70 inch (no diffuser) nozzle.

The test hardware assemblies were mounted in a high pressure pipe section. The testing assembly was rated for operation at 5000 psi. A photograph showing the Circuit A flow model being installed in the pipe section is contained in figure 8. A photograph of an assembly after a typical test is shown in figure 9.

## TEST PROGRAM

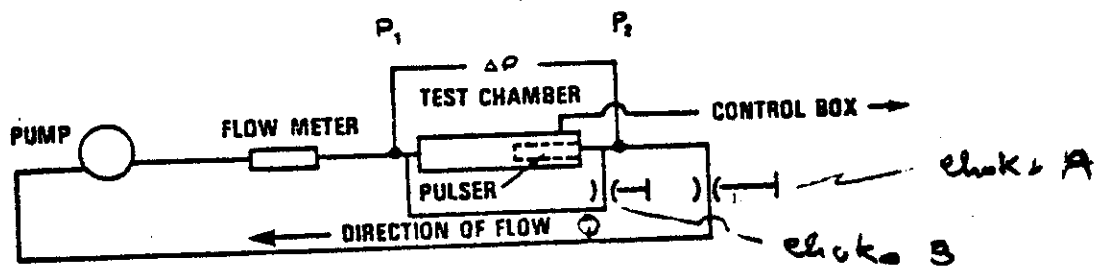
The test program was designed to quantify the effective flow areas and frequency response of each test circuit. The tests were conducted at the Terra Tek Drilling Research Laboratories using water and two drilling muds as the working fluids. The effects of fluid properties and nozzle design on the port area characteristics of each valve were measured.

The tests were performed using the set-up shown in figure 10. A typical test run consisted of circulating the drilling fluid through the test units for a period of 10 seconds while measurements were made of differential pressure and flow rate. Choke A was adjusted to provide a flow area representing a drill bit nozzle.

During the constant flow tests the flow rate and pressure were measured with the test circuit set to operate in either the vortex or nonvortex mode with choke <sup>B</sup> closed. The measurements were used to calculate the effective flow areas exhibited by each circuit configuration as a function of flow rate.

The response measurements were made with choke <sup>B</sup> partially open. This was done to maintain the differential pressure rise across the test circuit to within 500 psi for the purpose of protecting the pump. Under this condition the flow rate through the test unit varied approximately  $\pm 10\%$ . The response measurements were recorded on a digital data acquisition system. The measurements represent the change in differential pressure across the test unit due to the vortex action.

During a typical run, a variable frequency (0-8 Hz at 24 volts) electrical signal was applied across the solenoid coils. The change in differential pressure was recorded as a function of time during 10 second intervals. The data was played back with expanded time scales in order to measure response time.



MEASUREMENTS:

$Q$ - FLOW RATE	gpm
$\Delta P$ - PRESSURE DROP	psi
$\rho$ - DENSITY	ppg

Figure 10 Test setup.

## RESULTS

The effective flow area per stage is shown plotted as a function of flow rate per stage in figure 11. The flow areas indicated were calculated using equation 1.

$$A = \frac{Q}{109.5 \sqrt{\frac{\Delta p}{\rho}}} \quad (1)$$

where A = effective area (in<sup>2</sup>)

Q = measured flow rate (gpm)

$\Delta p$  = measured pressure (psi)

$\rho$  = density of the test fluid ppg.

Flow turn down was determined from the average values of effective flow area over the indicated range of flow rates per stage. Turn down data is summarized in Table I. The data plotted in figure 11 indicates that the effective flow area of a given circuit was for all practical purposes constant with flow rate and relatively unaffected by fluid composition. Circuit A with a convergent 0.70 inch diameter nozzle exhibited the highest turn down ratio (4:1) and an effective flow area equal to 0.272 in<sup>2</sup> (max). It can be seen from the data that the addition of a 0.875 in. diffuser raised the effective flow of the 0.272 in<sup>2</sup> area to 0.302 in<sup>2</sup> (max) while slightly reducing turndown ratio to 3.8.

Circuit B exhibited an effective flow area equal to approximately 0.40 in<sup>2</sup> (max) at a turn down ratio of approximately 2.7. The increase in effective flow area Circuit B compared to Circuit A is attributed to the absence of an amplifier.



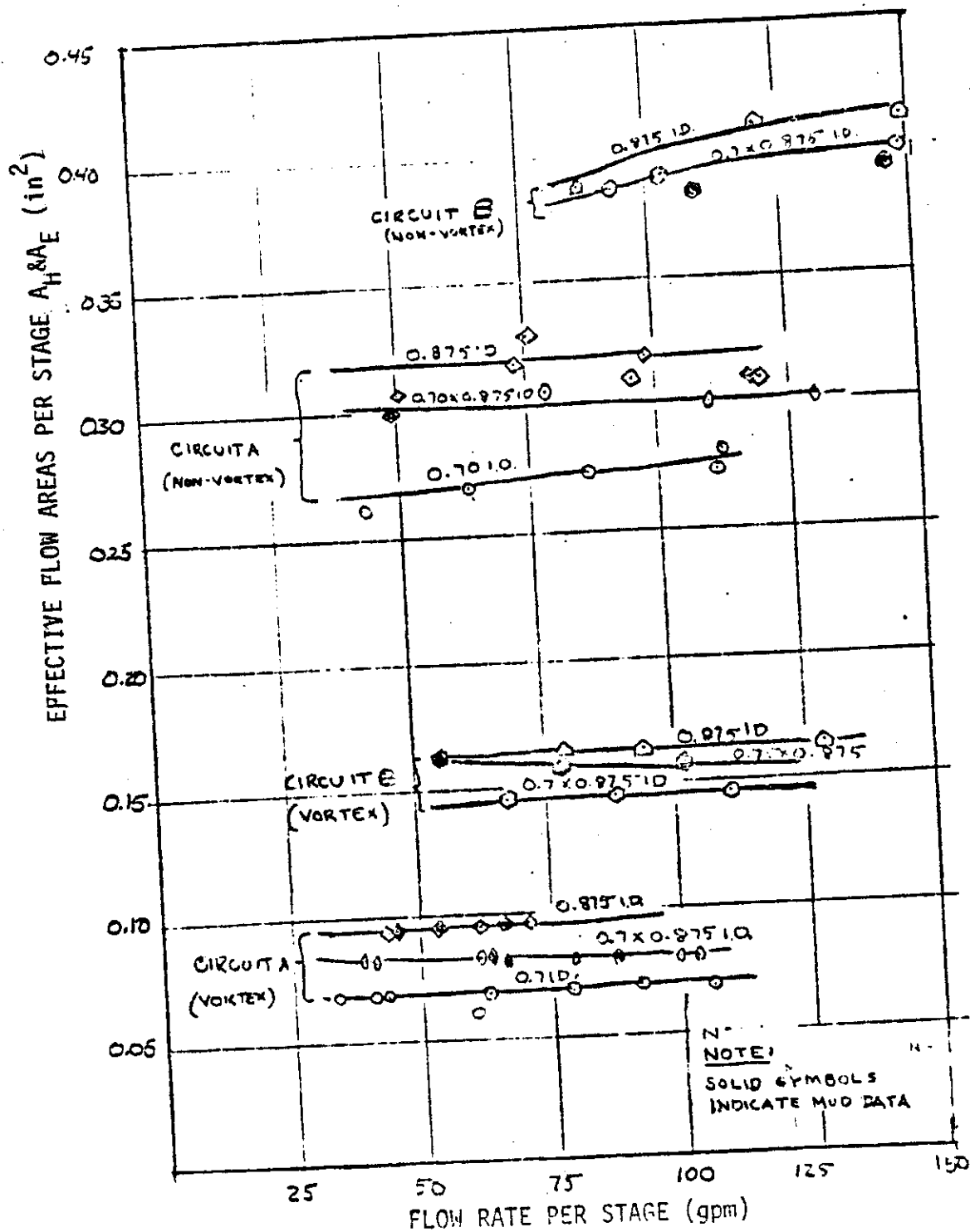
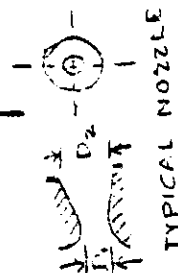


Figure 11 Calculated flow areas from test data.

TABLE 1

## SUMMARY OF TEST RESULTS

TEST CIRCUIT	NOZZLE DIAMETER		NOZZLE AREA		EFFECTIVE AREA: $A_E$ IN <sup>2</sup>	EFFECTIVE AREA: $A_H$ IN <sup>2</sup>	TURNDOWN RATIO
	$D_1$ IN.	$D_2$ IN.	$A_1$ IN <sup>2</sup>	$A_2$ IN <sup>2</sup>			
A	0.875	SAME	0.600	SAME	0.316	0.094	3.4
A	0.700	0.875	0.385	0.600	0.30	0.085	3.8
A	0.70	SAME	0.385	SAME	0.272	0.067	4.1
A	0.60	0.875	0.283	0.60	0.271	0.069	3.9
B	0.875	SAME	0.600	SAME	0.403	0.162	2.5
B	0.700	0.875	0.385	0.600	0.393	0.144	2.7



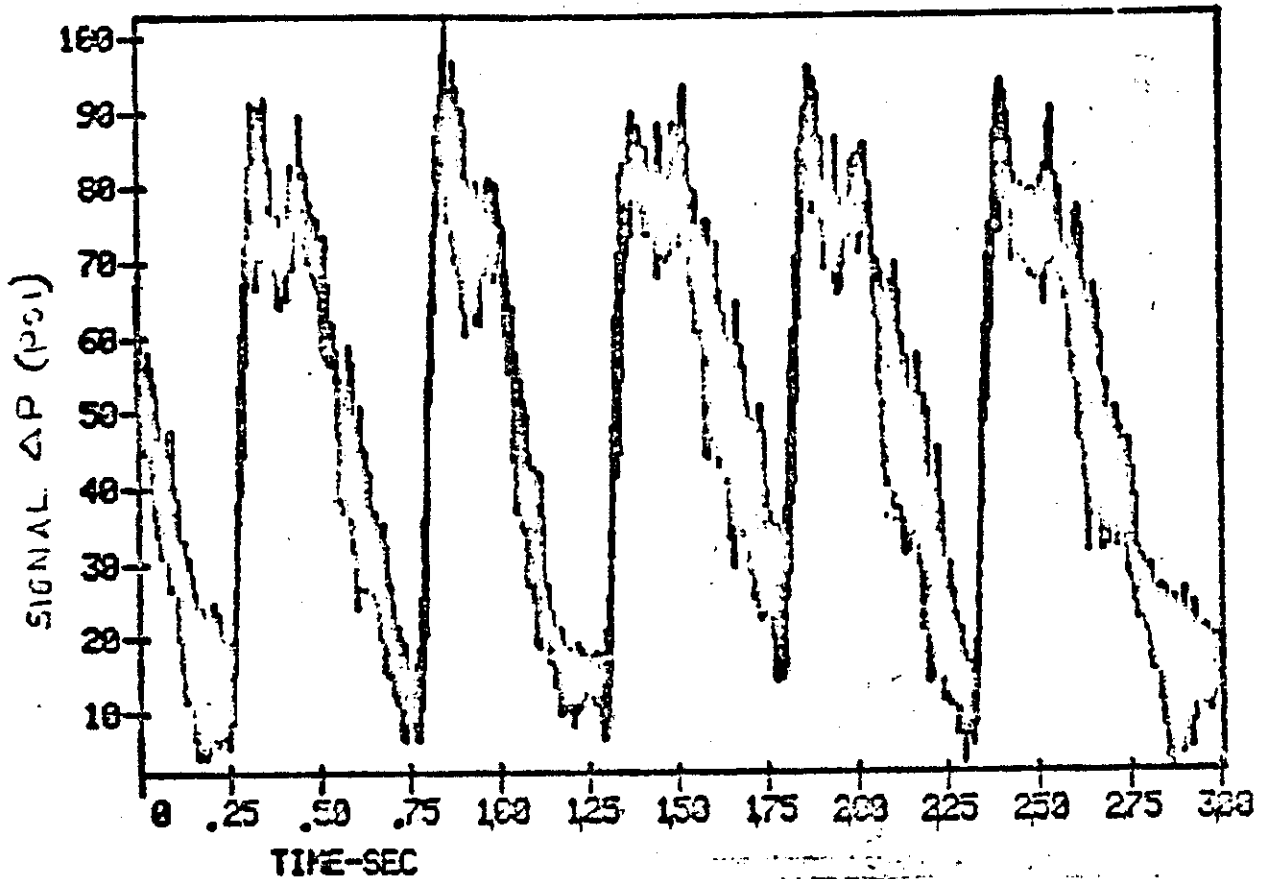
The response of circuits A and B to a (1 to 8 Hz) input voltage is illustrated in figures 12 through 15. Figure 12 describes the operation of Circuit A during three seconds at 2 Hz and 40 gpm/stage. Figure 13 describes the response characteristics of Circuit A during one second at 114 gpm/stage. A rise time of 0.04 seconds and a decay time of 0.18 seconds are indicated by the slope of the data plot shown in figure 13.

The response of Circuit B is illustrated in figures 14 and 15. Figure 14 describes the operation of Circuit B at 1 Hz and 100 gpm/stage during a 10 second run. Figure 15a describes the operation of Circuit B at 8 Hz and 125 gpm/stage during a 10 second run. Figures 15b and 15c describe this test run on expanded time scales. A rise time of 0.018 seconds and a decay time equal to 0.040 seconds was determined from the average slope of the traces contained in figure 15c.

The results clearly showed Circuit B to respond faster to control input signals than Circuit A. The relatively longer response time of Circuit A is attributed to a relatively complex but as yet undefined interaction between the amplifier and the vortex valve. The maximum frequency response of Circuit A was approximately 1.5 Hz.

Circuit B operated up to the maximum frequency (8 Hz) of the solenoid valve assemblies. The data indicates that the valve would have responded to higher frequency inputs had they been available. This conclusion is based on the measurements of the combined rise and decay time (0.058 seconds) as indicated in figure 15c.

\*\*\*ORLPLT\*\*\* X: TIME-SEC Y: LCH AP XCOL: 3 YCOL: 7  
 TESTID: FLUIDIC PULSER 5/7/89  
 \* QUICK \* FILE 5/7/89 03:23:51 TIME: 0.000- 3.000  
 RANGE X: 0.0000E+01- 2.9982E+03 Y: 1.8183E+00- 1.0637E+02  
 Y (A-D CHNL/ZERO/OFFSET/CAL): 57/-0.019/ 0.000/ 5.2263E+01



- Figure 12. Circuit A operating at 40 gallons per minute per stage between 0 and 3 seconds at approximately 2 hz.

\*\*\*ORLPLT\*\*\* X: TIME-SEC Y: LOW AP XCOL: 3 YCOL: 7  
 TESTID: FLUIDIC PULSER 5/7/88  
 \* QUICK \* FILE 5/7/88 08:23:51 TIME: 0.000- 1.000  
 RANGE X: 0.0000E-01- 9.9931E-01 Y: 4.3671E+01- 4.6443E+02  
 Y (A-D CHNL/ZERO/OFFSET/CAL): 57/-0.819/ 0.000/ 5.2253E+01

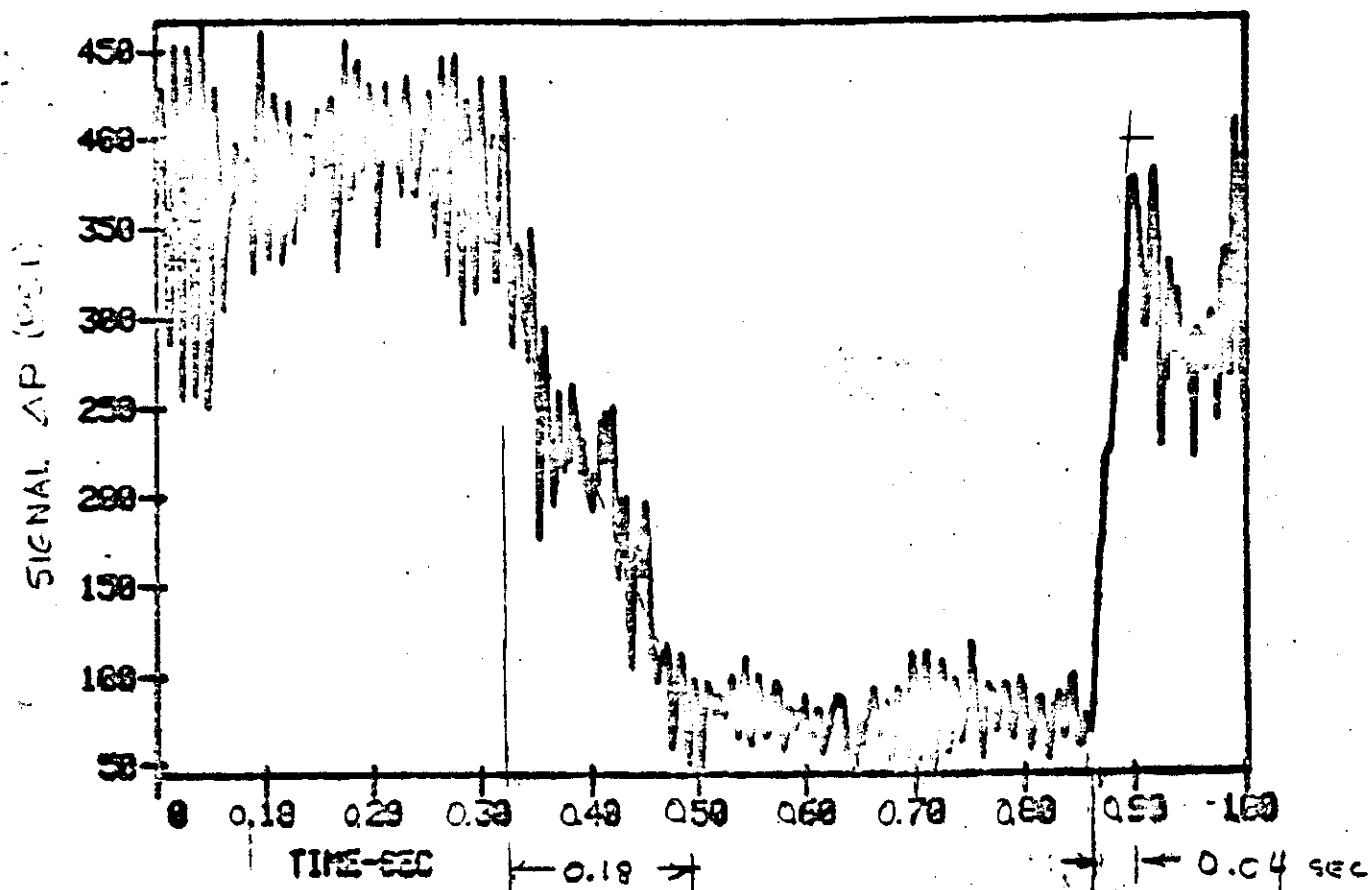


Figure 13 Circuit A operating at approximately 114 gpm/stage  
 with a 0.7 x 0.875 inch nozzle.

\*\*\*ORLPLT\*\*\* X: TIME-SEC Y: LOW AP XCOL: 3 YCOL: 7  
 TESTID: VORTEX 5/7/88  
 \* QUICK \* FILE 5/7/88 11:11:54 TIME: 0.000- 18.000  
 RANGE X: 0.0000E+01- 9.9977E+00 Y: 4.3207E+01- 3.8130E+02  
 Y (A-D CHNL/ZERO/OFFSET/CAL): 57/-0.024/ 0.000/ 5.22346E+01

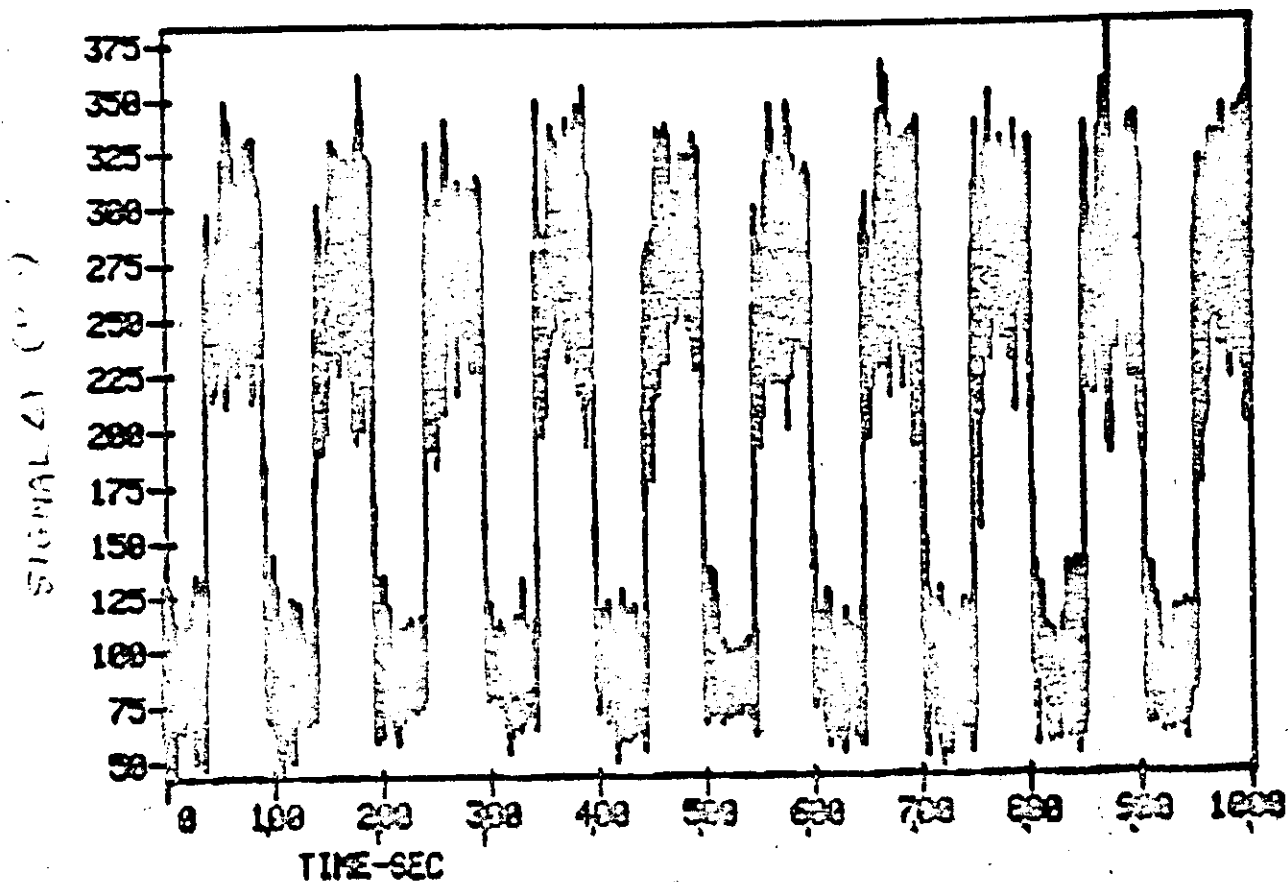


Figure 14. Circuit B operating at approximately 100 gpm/stage  
 with a 0.7 x 0.875 inch nozzle, at 1 Hz.

\*\*\*ORLPLT\*\*\* X: TIME-SEC Y: LOW AP XCOL: 3 YCOL: 7  
 TESTID: UCRTX 5/7/80  
 \* QUICK \* FILE 5/7/80 11:11:54 TIME: 0.000- 10.000  
 RANGE X: 0.0000E+01- 9.9977E+00 Y: 3.2825E+00- 4.3400E+02  
 Y (A-D CHNL/ZERO/OFFSET/CAL): 57/-0.024/ 0.000/ 5.2234E+01

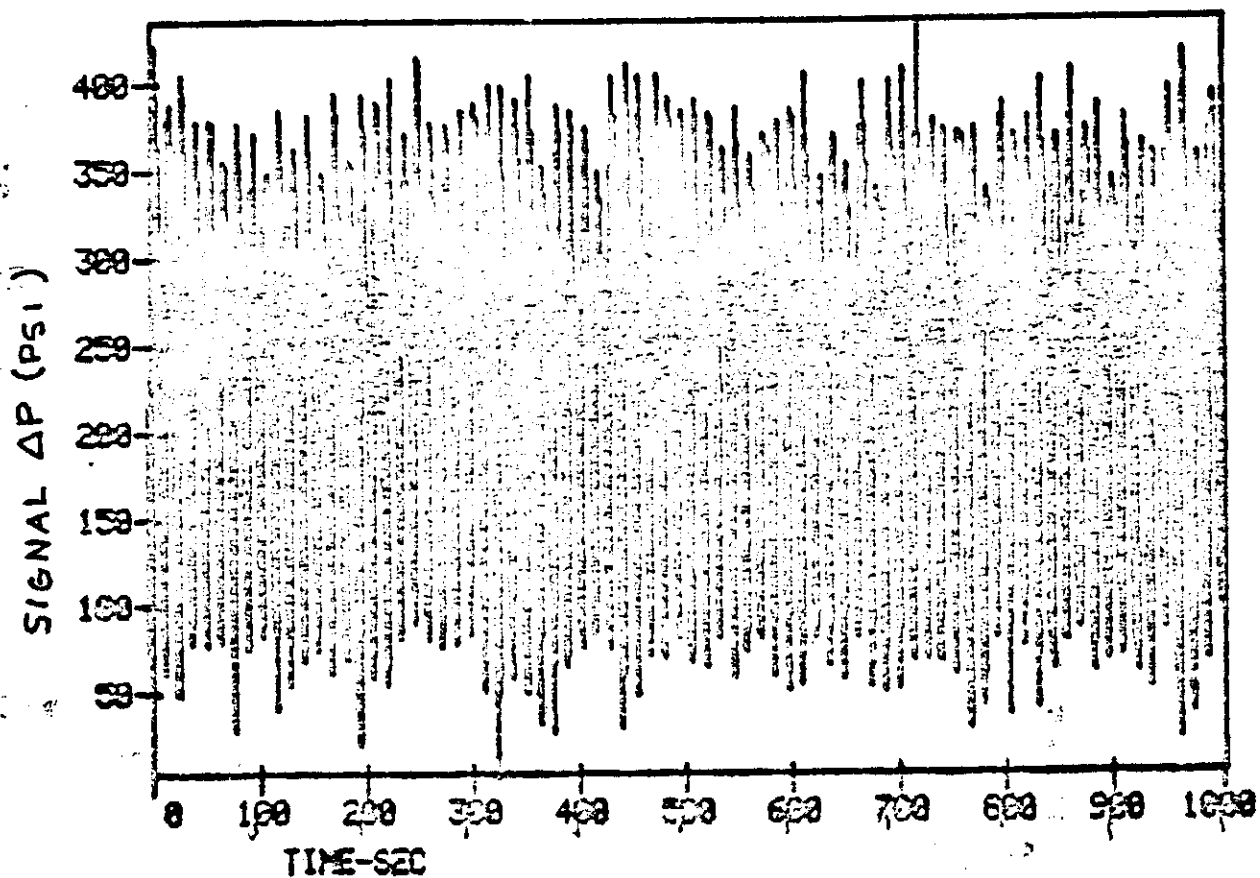


Figure 15a Circuit B operating at 125 gpm/stage with a  
 0.7 x 0.875 inch nozzle (at 8 Hz).

\*\*\*ORLPLT\*\*\* X: TIME-SEC Y: LOW AP XCOL: 3 YCOL: 7  
 TESTID: VORTEX 5/7/80  
 " QUICK " FILE 5/ 7/80 11:11:54 TIME: 3.800- 4.800  
 RANGE X: 3.000E+00- 3.999E+00 Y: 3.222E+00- 4.016E+02  
 Y (A-D CHNL/ZERO/OFFSET/CAL): 57/-0.624/ 0.000/ 5.2234E+01

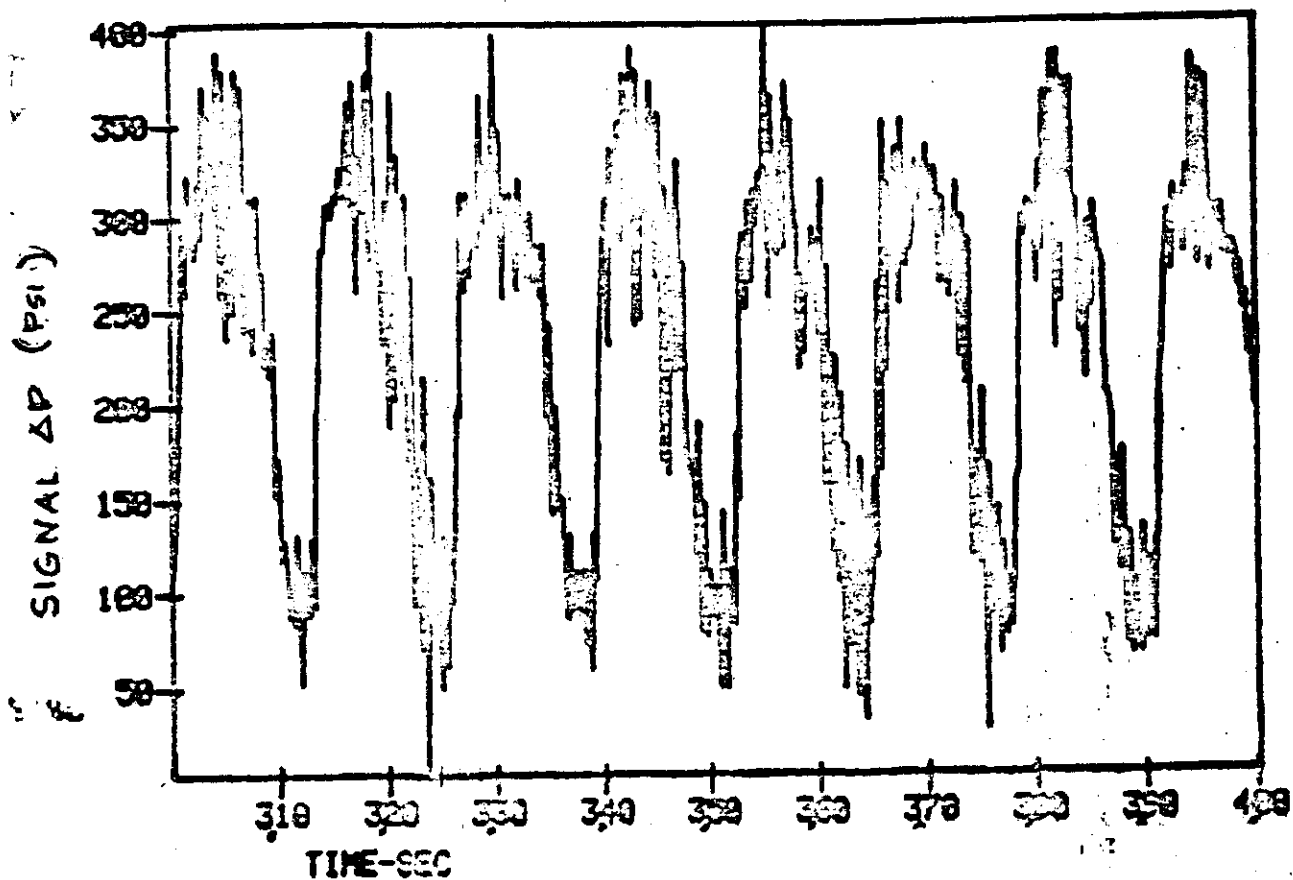


Figure 15b Circuit B operating at 125 gpm/stage with a  
 0.7 x 0.875 inch nozzle (at 8 Hz).



\*\*\*ORLPLT\*\*\* X: TIME-SEC Y: LOW AP XCOL: 3 YCOL: 7  
 TESTID: VORTEX 5/7/80  
 " QUICK " FILE 5/7/80 11:11:54 TIME: 3.700- 3.900  
 RANGE X: 3.7018E+00- 3.8996E+00 Y: 2.8341E+01- 3.8554E+02  
 Y (A-D CHNL/ZERO/OFFSET/CAL): 57/-0.024/ 0.000/ 5.2234E+01

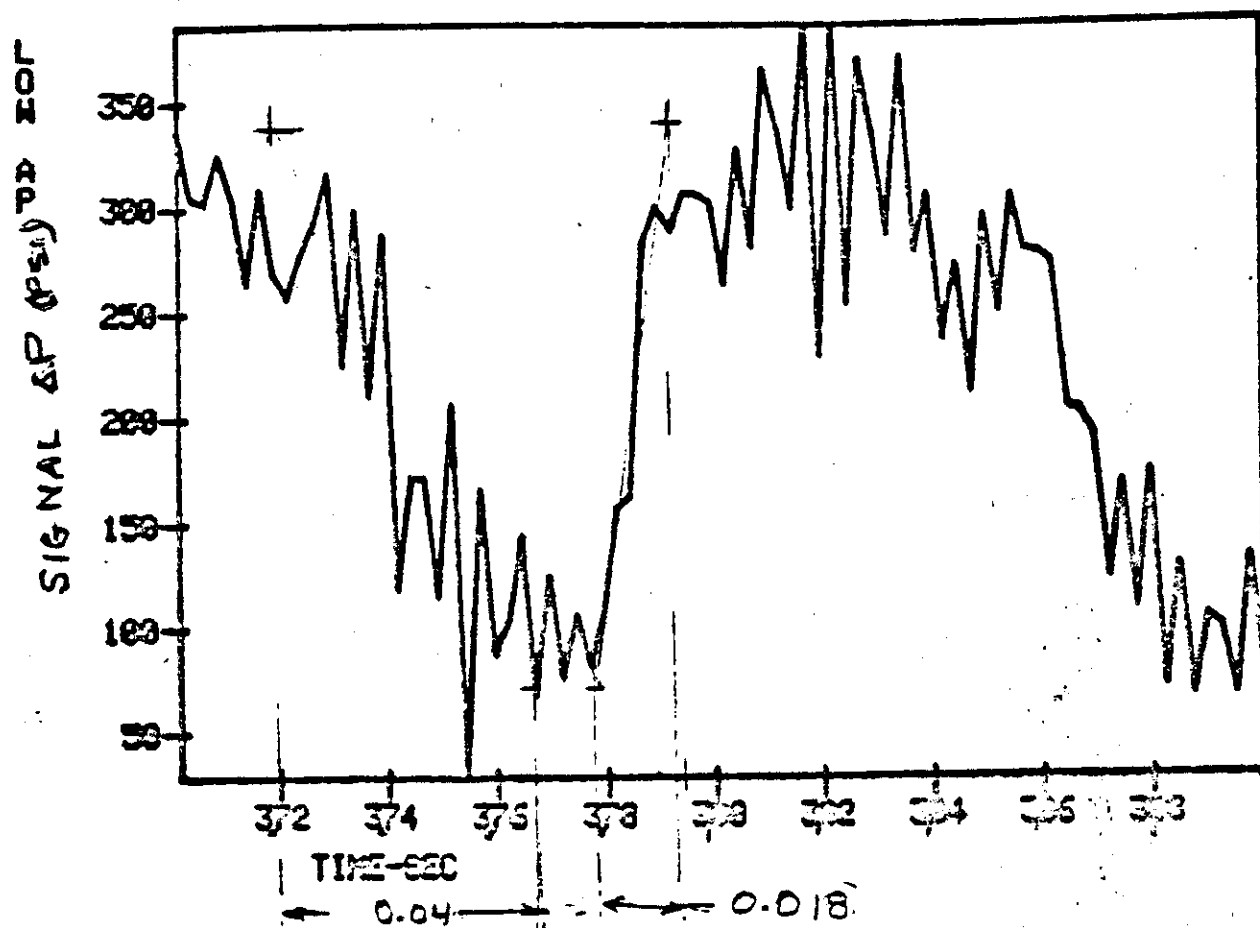


Figure 15c Circuit B operating at 125 gpm/stage with a  
 0.7 x 0.875 inch nozzle (at 8 Hz).

## DISCUSSION

In the previous section measurement data was presented describing the effective flow areas and change in flow areas of individual pulser stages. This section describes how these port area characteristics can be used to calculate signal amplitude and operating pressure drops in a circulating system. The effects of turn down ratio on signal efficiency (defined as the ratio of the signal pressure to the average operating pressure drop required to produce the signal) is discussed. An illustrative problem is given describing how to select the optimum number of valving stages for a given set of circulating flow conditions.

The flow equations which govern the operation of a pulser valve in a circulating system are developed in Appendix A. The analysis procedures describe a valve operating in series with a drill bit nozzle and in parallel with a bypass. For the analysis it is assumed that the valve is operated at a pulse rate fast enough so that an individual pulse does not have time to travel to the pump and back before the next pulse is initiated. It is also assumed that the valve spends an equal amount of time in the open and shut down state. These assumptions were made so that average flow conditions could be assumed.

The curves plotted in figure 16 represent the signal pressures and operating pressure drops which would be produced by any valve with the indicated port areas operating under the conditions specified. The change in signal and operating pressure due to the addition of a bypass is determined by adding the bypass area to the valve areas. The curves also show that signal efficiency does not vary much along the lines of constant turn down. Using the values of

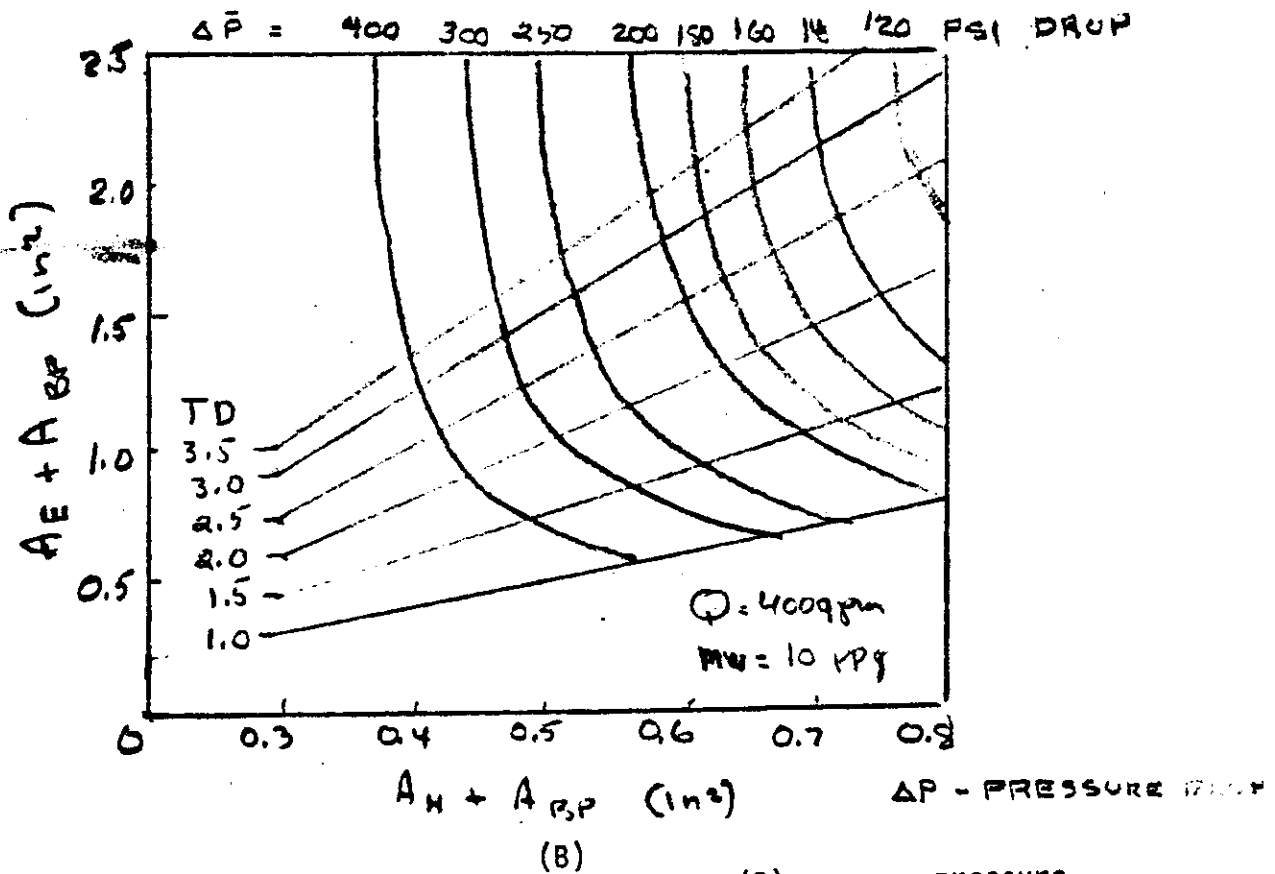
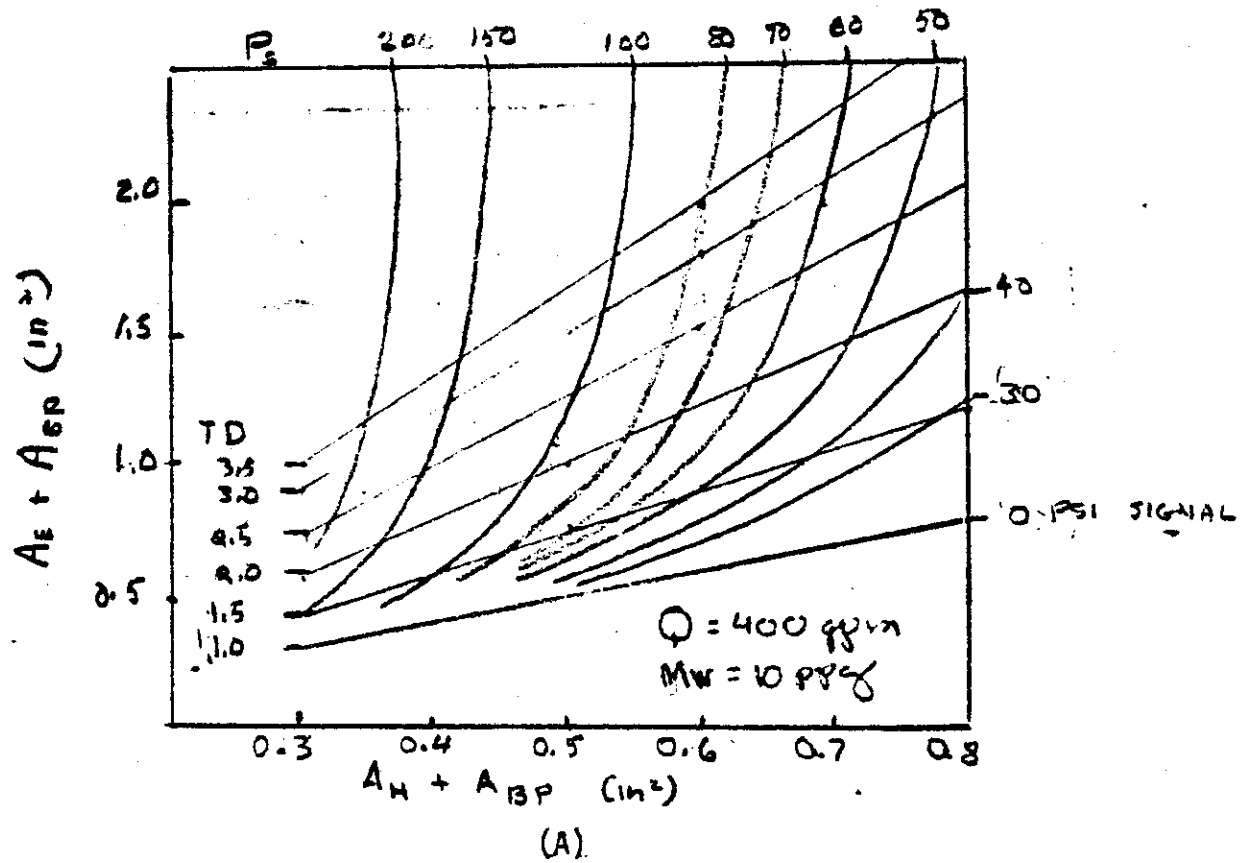


Figure 16 Calculated (A) signal pressure, (B) average pressure across given combinations pulser flow areas and by-pass areas. Calculations are based on a drill pipe internal diameter = 3.75 in, nozzle bit area = 0.36 in<sup>2</sup>. Circulation rate = 400 gallons per minute, mud weight 10 pounds per gallon and a sound speed in mud = 3700 feet per second.

signal pressure and pressure drop it is possible to replot the data to illustrate the effect of turn down on signal efficiency. The curve (figure 17) shows that the point of diminishing returns (indicated by the change in slope) is reached at a turn down ratio of approximately 3/1. This means that little is to be gained by operating at turn down ratios much above 3/1. The only possible advantage would be the optional use of a bypass to reduce pressure drop while maintaining the effective system turn down  $(A_E + A_{\text{bypass}}) / (A_H + A_{\text{bypass}}) = 3$ .

To further illustrate the use of these curves let it be assumed that a 4-stage fluidic valve is to be used under the conditions stated above and that the user has the option of employing any number of active stages as well as a bypass. -Let it be further assumed that each stage has operating characteristics equal to those of a B-type circuit with a 0.7 x 0.875 inch nozzle.

The maximum and minimum effective flow areas indicated for this B-type circuit stage (Table 1) are 0.40 and 0.15 in<sup>2</sup>. Multiplying these values by the number of stages gives the equivalent values for a 2, 3 and 4 stage valve. These values are represented by points 2, 3 and 4 in figure 18. The lines extending to the right of each point describe the pressure associated with the addition of bypass flow area.

#### OTHER CONSIDERATIONS

The optimum combination signal pressure and pressure drop depends upon other factors in a circulating system which have yet to be determined. Of these, the amplitude attenuation of the signal with hole depth mud properties and pulse frequency are most important. Appendix B contains a theoretical

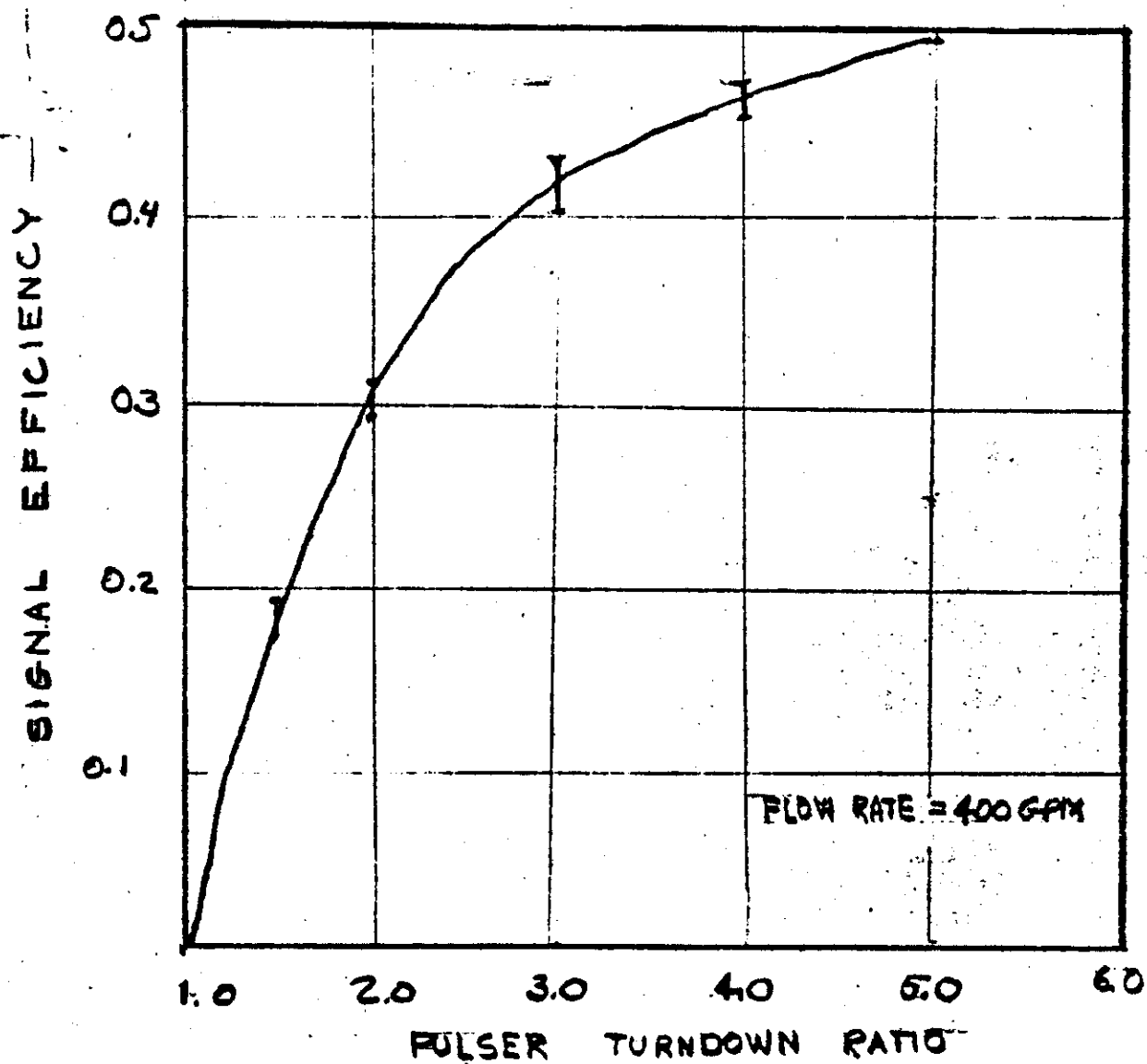


Figure 17 Signal efficiency (plotted from data on figure 16.)  
as a function of turn down.

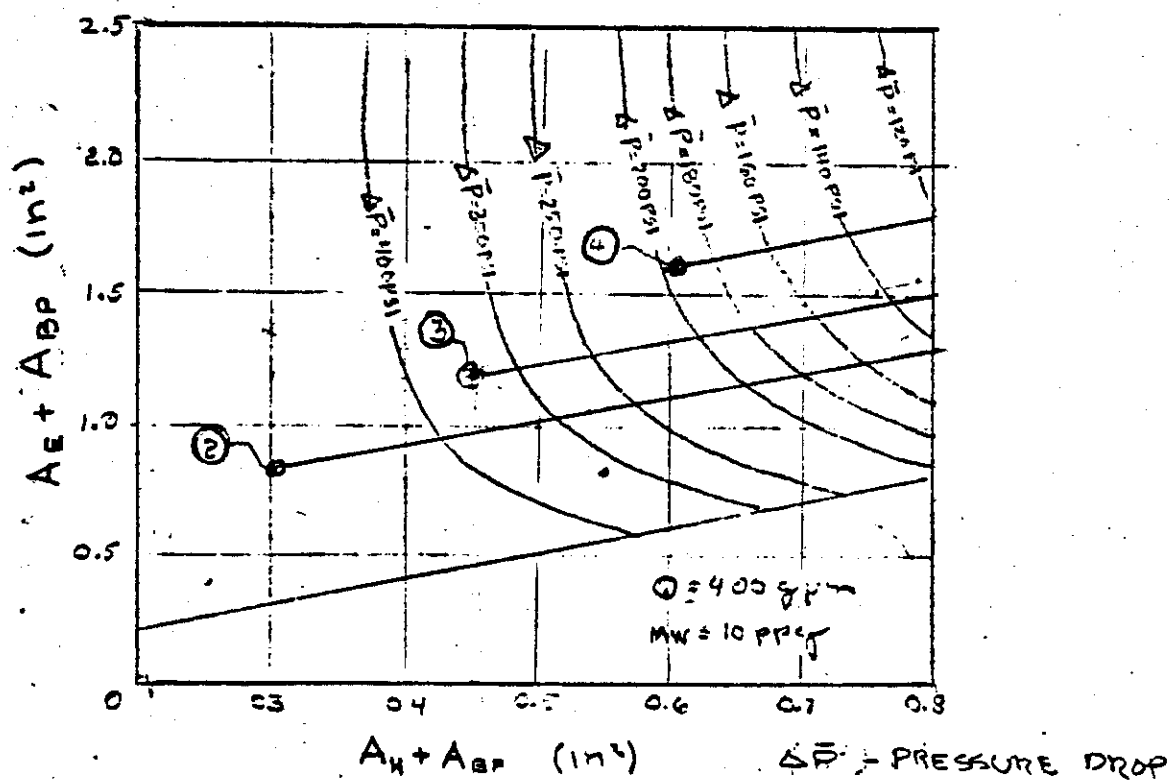
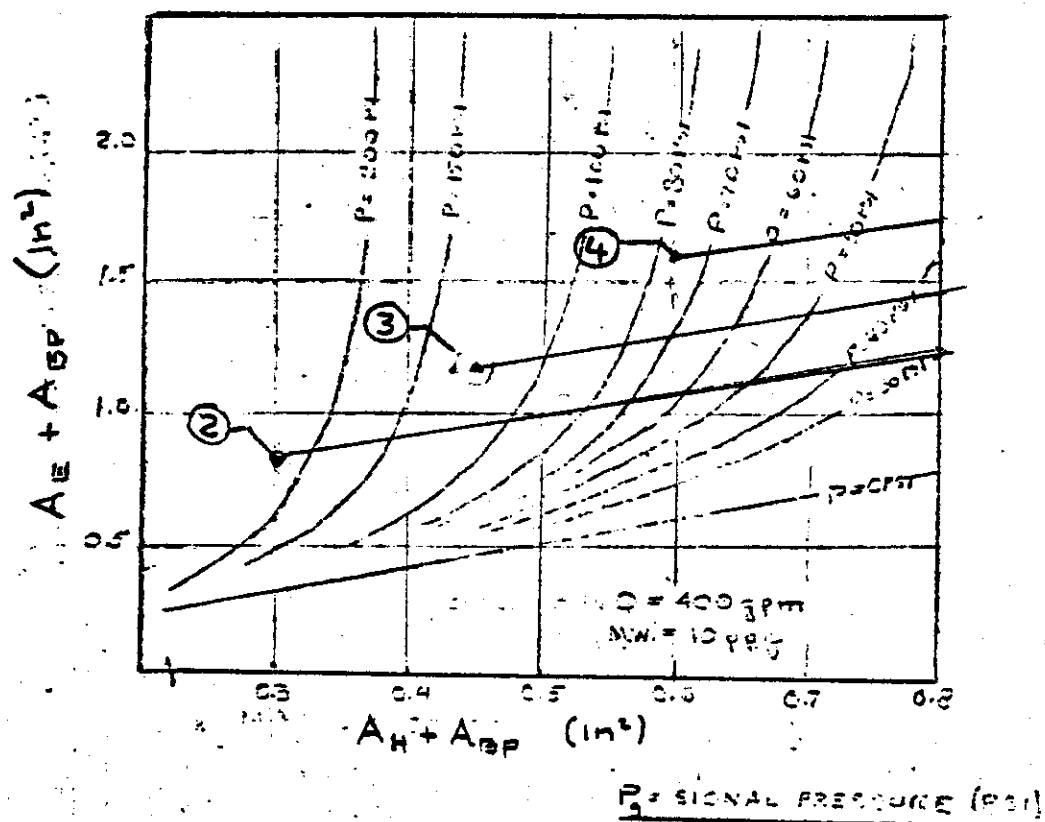


Figure 18 Data replotted from figure 16 to illustrate the operating points for a 2,3 and 4-Stage (B-Type) pulser with a by-pass.

analysis of mud pulse attenuation. The analysis is based on the classical hydrodynamic derivations presented by Lamb. Although experimental data is needed to confirm this theory, particularly where the dispersive and compressibility properties of the drilling mud and the circulating system may <sup>a</sup>effect wave propagation, it is presented here for comment and discussion.

The results of the analysis are summarized in figure 19. The figure represents a graphical solution to Lamb's equations given in Appendix B for calculating half depth. The analysis procedures provide a first approximation of the distance (d) where the amplitude of the pressure pulse produced by a pulser is attenuated to 1/2 its original value. To determine half depth from the graph in figure 19, four quantities must be known: pulser frequency (f) mud viscosity ( $\nu$ ), minimum diameter in the drill pipe (d) and acoustic velocity in the mud (C).

To illustrate the use of the graph, the following quantities have been assumed:

$$f = 10 \text{ Hz} = 10 \times 60 = 600 \text{ RPM}$$

$$d = 2.5 \text{ in. internal diameter of a tool joint in a } 4 - 1/2 \text{ in drill pipe}$$

$$C = 4300 \text{ ft/sec}$$

$$\nu = 10 \text{ cs}$$

Enter graph at the top with  $f = 600 \text{ rpm}$ . Go to the  $\nu = 10$  line. To correct for pipe diameter and sound velocity, calculate the product  $d \times c = 10750$ ; move horizontally right to the point approximating this value. Read half depth (D) = 4500 ft or lower scale.

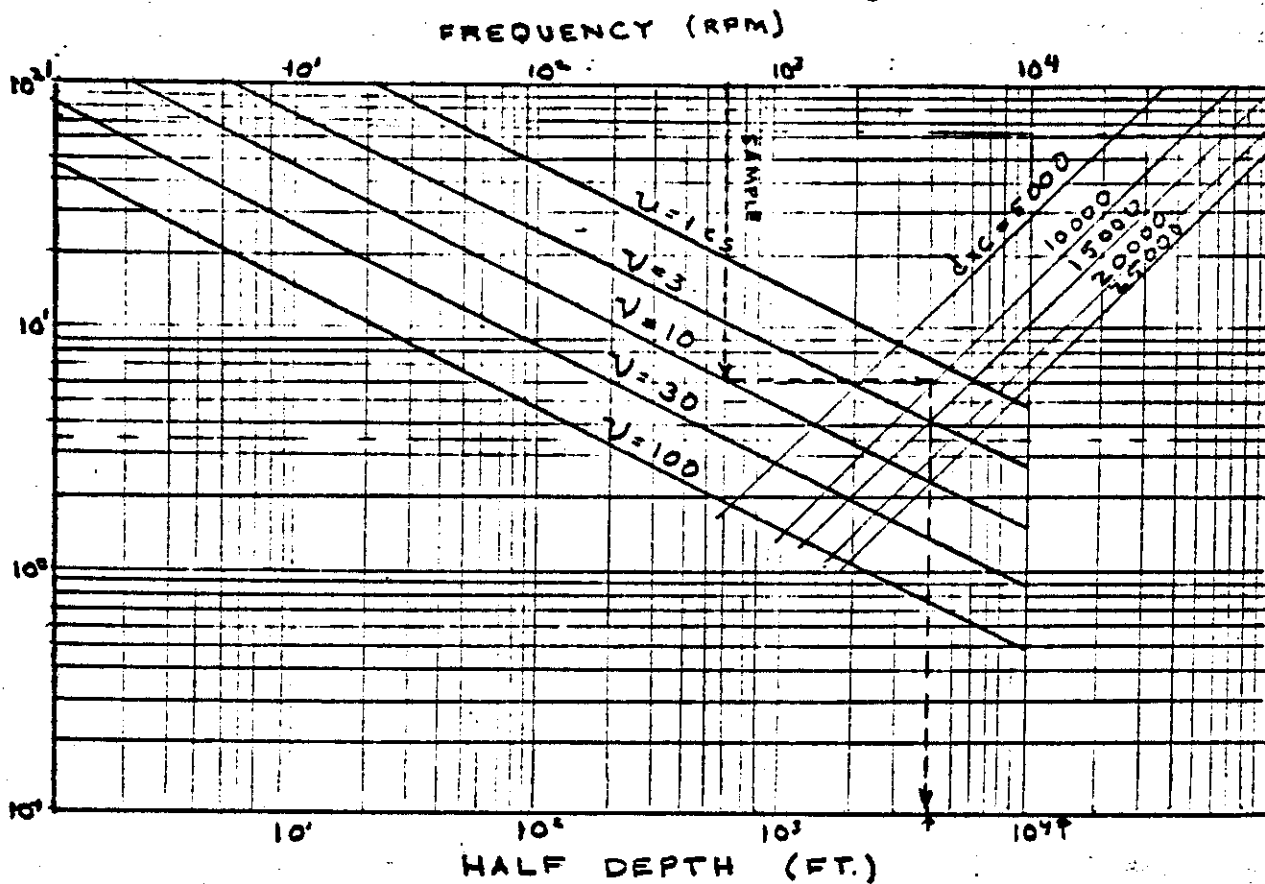


Figure 19 Nomograph for determining half depth.



## SUMMARY AND CONCLUSIONS

Fluidic techniques have been applied to the design of a valve for mud pulse telemetry applications. Flow tests have demonstrated that a fluidic valve has the capability to operate from 10 to 20 Hz at 400 gpm with an average pressure drop of 325 psi on 10 ppg mud. The amplitude of the signal under the assumed operating conditions is 125 psi. A first approximation of the half depth showed that (at 10 Hz) this signal would be attenuated by <sup>50 %</sup> ~~60 psi~~ at well depths ranging between 4000 to 10,500 ft over a mud viscosity range of 1 to 10 centistokes for the circulating conditions assumed.

Although the results of the attenuation analysis have not been verified experimentally, it is concluded that the type and degree of performance attainable through the application of fluidic control technology to mud pulse valve design will cover a wide range of mud pulse telemetry requirements.

## APPENDIX A

### MUD PULSE TELEMETRY FLOW ANALYSIS

## MUD PULSING (Operating Principles)

In a mud pulse telemetry system, signals are generated down hole by inducing momentary local changes in flow rate through the drill string. The change in flow rate is accomplished by rapidly changing the flow resistance of the pulser-bit nozzle, ~~in the~~ ~~at the~~ ~~on~~.

If the pulser is far enough away from the mud pump so that pressure waves require longer to make the round trip from the pulser to the pump and back than for the valve to complete actuation, then a change in flow rate and static pressure occurs as a result of the change in flow resistance. For an increase in resistance, the adverse pressure gradient which exists across the generated wave can be viewed as the force which is required to slow the incoming flow; conversely, the increase in static pressure can be viewed as storing the kinetic energy lost by the fluid as it passes through the wave. The relationship between the change in pressure ( $P_1 - P_2$ ) and the change in flow rate ( $Q_1 - Q_2$ ), called the water-hammer relationship, is given by

$$(Q_1 - Q_2) = -K (P_1 - P_2) \quad (1)$$

where  $P_1$  and  $Q_1$  are the high resistance pressure and flow rate,  $P_2$  and  $Q_2$  are the low resistance pressure and flow rate, and  $K$  is a proportionality constant given by  $K = A/\rho c$ , where  $A$  is the drill string cross-sectional area, and  $\rho$  and  $c$  are the density and sound speed for the drilling fluid.

If the pulser flow resistance is rapidly changed and then maintained at the new condition for a substantial time (several acoustic-wave transit-times), then the flow rate will return to the original value (assuming a constant flow mud pump) as the reflected pressure waves build up the pressure upstream of the pulser. Assuming the valve actuation causes an increase in flow resistance, the pressure upstream of the pulser will rapidly increase by the amount determined by the waterhammer relationship. As the reflected pressure waves arrive at the pulser, the pressure rises to the steady-state

value associated with the higher resistance of the pulser-bit nozzle combination.

If the pulser is repeatedly switched between its two states in rapid succession as it would be when transmitting a coded series of pulses, the pressure and flow upstream of the pulser will be switched between two relatively steady values. The average flow rate through the drill string must be the same as the pump flow rate since the inertia of the pump and compliance of the circulating system will not follow the rapid changes of the pulser. If it is assumed that the pulser spends an equal amount of time in each of its two states, then the average flow rate through the drill string upstream of the pulser will be  $(Q_1 + Q_2)/2$ . Thus, if the pump flow rate is  $Q_0$ , then

$$Q_1 + Q_2 = 2Q_0. \quad (2)$$

In a mud pulsing system the pulser valve forms a series resistance with the bit nozzle. The signal (waterhammer pressure wave) is generated as the pulser effective area is switched between two values,  $A_H$  and  $A_E$ , or the "hard" and "easy" areas. The bit nozzle area is represented by  $A_3$ . In all calculations, <sup>which follow</sup> in this report, the bit area is adjusted by a discharge coefficient of 0.952. In this way all pressure drop calculations for the bit agree with standard hydraulic tables and slide rules used by the industry. *dash put spaces each side* Whenever an area is stated for the bit, it is the actual bit nozzle throat area-not an effective area. Failure to note this procedure can cause almost 10 percent error in pressure drop calculations.

Because the pulser is in series with and upstream of the drill bit, the following equations relate the flow rate to the pressure drop across the pulser and bit nozzles (pressure downstream of the bit nozzles is assumed constant and all pressures are referenced to it):

Pulser pressure drop,

$$Q_1^2 = K_1^2 (P_1 - P_{B1}), \text{ Hard} \quad (3)$$

$$Q_2^2 = K_2^2 (P_2 - P_{B2}), \text{ Easy} \quad (4)$$

Bit nozzle pressure drop,

$$Q_1^2 = K_3^2 (P_{B1}), \quad \text{Hard} \quad (5)$$

$$Q_2^2 = K_3^2 (P_{B2}), \text{ Easy} \quad (6)$$

For the two pulser states,  $K_1 = A_H \sqrt{ZT\rho}$ ,  $K_2 = A_E \sqrt{ZT\rho}$ ,  $K_3 = 0.952 A_3 \sqrt{ZT\rho}$ , and  $P_{B1}$  and  $P_{B2}$  are the pressures between the pulser and the bit. These six equations--(1) through (6)--have six unknowns,  $Q_1$ ,  $Q_2$ ,  $P_1$ ,  $P_2$ ,  $P_{B1}$  and  $P_{B2}$  so

they uniquely describe the flows and pressures at the pulser and bit when the pulser effective areas,  $A_H$  and  $A_E$ , the bit area,  $A_3$ , and the average flow rate,  $Q_0$ , are given.

When these equations are solved for  $Q_2$ , a quadratic equation results, the solution of which is

$$Q_2 = \frac{-b \pm \sqrt{b^2 - 4ac}}{2a} \quad (7)$$

$$a = (1/K_{23}^2)(1/K_{13}^2)$$

$$b = (2/K) + (4Q_0/K_{13}^2)$$

$$c = - [(4Q_0^2/K_{13}^2) + (2Q_0/K)]$$

$$(1/K_{13}^2) = (1/K_1^2) + (1/K_3^2)$$

$$(1/K_{23}^2) = (1/K_2^2) + (1/K_3^2)$$

The remaining five unknowns,  $Q_1$ ,  $P_1$ ,  $P_2$ ,  $P_{B1}$ , and  $P_{B2}$  can be found readily from equations (1) through (6) once  $Q_2$  is known.

P. 11-5

## Graphical Representation Techniques

An examination of equations (1) through (7) shows that signal levels, flows and pressure drops through an operating series pulser depend on the two pulser effective areas, bit area, mud pump flow rate, drill string cross sectional area, mud density and sound speed--a total of seven variables. Parameters of interest to drilling operations are waterhammer signal level, average pressure drop across the pulser, average pressure drop across the bit, and average flow rate through the bit. At first these variables and parameters present a bewildering array of possibilities, with little hint of how to choose the pulser effectiveness areas and the bit area--the three variables over which one has some control--in order to produce a required signal level while still optimizing bit hydraulics for maximum bottom-hole cleaning.

Some of the variables may be eliminated from consideration. Sound speed in the drilling fluid is probably constant enough to cause little change in pulser design. Mud density may be factored out of each of the equations involving pressure drops so that calculations at 10 ppg of the various pressures of interest may be converted to any other fluid density by multiplying all pressures by  $\rho/10$ , where  $\rho$  is measured in pounds per gallon. Drill string cross sectional area is a parameter which strongly affects signal level because it determines the average velocity in the drill string (as in equation (1)). Pressures calculated at one drill string area are the same as those for a different drill string area if all other areas and flows are similarly scaled.

The parameters of major interest in drilling operations are signal pressure level and average pressure drop across the pulser valve. The average bit pressure drop is approximately the same as the bit pressure drop at the average flow rate, that is,  $Q_0/K_3$ . The exact value is given by  $1/2 [(Q_1/K_3) + (Q_2/K_3)]$ . If we define  $Q_1 = Q_0 - Q$  and  $Q_2 = Q_0 + Q$ , then the exact value reduces to  $(Q_0 + Q^2)/K_3$ . Because  $Q$  is normally less than  $0.1Q_0$ , the error in assuming that the average bit pressure drop is  $Q_0/K_3$ , is less than 1 percent. This approximation removes the dependence of average bit pressure drop on waterhammer signal level (proportional to  $\Delta Q$ ).

The signal pressure level,  $P_s$ , is defined by

$$P_s = P_1 - P_2 \quad (8)$$

The average pressure drop across the pulser,  $P$ , is defined by

$$P = 1/2 [Q_1/K_1 + (Q_2/K_2)], \quad (9)$$

that is, half the sum of the pressure drops across the pulser in the hard and easy flow modes. Note that this again assumes that, on the average, the pulser spends equal times in each of its two states. The ratio,  $P_s/P$ , may be viewed as the efficiency with which a pulser-bit nozzle combination generates the water hammer signal and will be called the signal efficiency.

Appendix B

MUD PRESSURE PULSE ATTENUATION

Prepared by

Dr. William J. McDonald

Dr. Donald W. Dareing

for

U. S. Harry Diamond Laboratories

March 1980



## TABLE OF CONTENTS

	Page
SUMMARY AND CONCLUSIONS.....	ii
TABLE OF CONTENTS.....	iii
INTRODUCTION.....	1
PRESSURE PULSE ATTENUATION THEORY.....	2
CALCULATIONS OF ATTENUATION "HALF DEPTHS".....	7
EMPIRICAL CALIBRATION OF THE THEORY.....	15
NOMOGRAM SOLUTION TO THE ATTENUATION CALCULATION.....	18

## SUMMARY AND CONCLUSIONS

A simple mud pressure pulse attenuation theory is presented. This theory is based on classical hydrodynamic derivations presented by Lamb, and is of a form

$$D = 35.3 \frac{d \times c}{\sqrt{f \times v}}$$

Where  $D$  = well depth that attenuates the mud pressure pulse signal to one-half its original strength.

$d$  = effective internal pipe diameter (inches)

$c$  = speed of sound in mud (ft/sec)

$f$  = pulse frequency (RPM)

$v$  = kinematic viscosity (cs)

The theory compares well with the limited experimental data available if the minimum pipe ID (that of the tool joint) is used for  $d$ , and the Bingham Plastic Viscosity,  $PV$ , is taken as a good approximation to the absolute viscosity.

Thus the theory is a good approximation for calculating pulse attenuation. However, additional experimental data should be obtained to further confirm the theory, particularly where the dispersive and compressibility properties of the drilling fluid and its flow system may show effect on wave propagation.

## INTRODUCTION

Several fundamental types of Measurements-While-Drilling (MWD) are under development including hard wire, acoustic, EM and mud pressure pulse systems. All systems have advantages and disadvantages. Mud pulse systems are under development by several groups. The work at Harry Diamond Laboratories offers potential for improvement of the mud pulse technology through development of a fluidics valve to generate the pulse.

The fluidics valve could have several advantages including (1) low power consumption, (2) high switching rate (potentially higher data rate), (3) simplified customizing for different flow parameters, (4) better control of valve erosion, and others.

Essential to proper design of a fluidics mud pulse system is an understanding of the attenuation of the pressure pulse in the drill string. Pipe size, fluid viscosity, and pulse rate all affect attenuation and spreading of the mud pressure pulse, and have affect on the detectability of the signal at the surface.

A simple, basic theory based on Lamb has been used in this report to help understand the mud pulse attenuation problem. While the theory does not account for properties such as compressibility and dispersion, the usefulness of this approach is confirmed by data acquired by Mobil in the development of their mud pulse system.

## PRESSURE PULSE ATTENUATION THEORY

Lamb\* has derived that the change in pressure amplitude for a wave traveling along a tube is given by:

$$p(x) = p_0 e^{-\frac{x}{\ell}}$$

where  $\ell = \frac{dc}{v\beta}$

and  $\beta = \sqrt{\frac{\sigma}{2v}}$

is a measure of the extent to which the influence of viscosity penetrates into the fluid.

Thus,  $\ell = dc \sqrt{\frac{2}{v\sigma}}$

where

- d - inside radius of pipe, (ft)
- c - speed of sound (ft/sec)
- v - kinematic viscosity of fluid, (centipoise)
- $\sigma$  - pressure pulse frequency (rad/sec)
- $\ell$  - distance in which amplitude falls to 1/e of its original value.

---

\*Lamb, Hydrodynamics, Dover (New York, N.Y.) 1945, pp 652-633 (see this report page 5).

Expressing parameters in terms of English and oilfield units

$$c = \sqrt{\frac{E}{.233\rho}} \quad \text{where } E = \text{bulk modulus lb/ft}^2 \\ \rho = \text{density, lb/gal}$$

$$\mu(\text{absolute viscosity, cp}) = \nu(\text{kinematic viscosity, cs}) \times \rho (\text{density, g/cc})$$

$$\text{Note: } 1 \text{ centipoise} = 1.45 \times 10^{-7} \text{ reyns } \left( \frac{\text{lb-sec}}{\text{in}^2} \right)$$

To convert  $\mu$  (absolute) to reyns

$$\mu = \mu(\text{cp}) \times 1.45 \times 10^{-7} \frac{\text{lb-sec}}{\text{in}^2}$$

$$\mu = \mu(\text{cp}) \times 1.45 \times 10^{-7} (144 \text{ in}^2/\text{ft}^2) \frac{\text{lb-sec}}{\text{in}^2}$$

$$\nu \left( \frac{\text{ft}^2}{\text{sec}} \right) = \mu(\text{cp}) \times 2.09 \times 10^{-5} \frac{\text{lb-sec}}{\text{ft}^2} \times \frac{g}{\rho} \\ = 1.075 \times 10^{-5} \times \nu(\text{cs})$$

also see Marks\* page 230-231

$$\sigma = 2\pi f \text{ rad/sec}$$

where  $f$  is pressure pulse frequency in Hertz

---

\*Marks, Mechanical Engineers' Handbook, McGraw-Hill, New York, 1951  
this report

The equation for damping of the pressure wave in a fluid may also be written in the form.

$$e^{\beta} = 2^{\alpha}$$

$$\beta \ln(e) = \alpha \ln(2)$$

where  $\alpha = \frac{\beta}{\ln(2)}$

Thus the pressure pulse equation can be written

$$p(x) = p_0 2^{-\frac{x}{\ln(2) \ell}} = p_0 2^{-\frac{x}{D}}$$

where

$$D = \ln(2) \times \ell$$

= the distance in which amplitude falls to 1/2 of its original value.

## CALCULATION OF ATTENUATION "HALF DEPTH"

Using the theory presented in the previous section, pressure attenuation expressed as attenuation "Half Depth" was calculated for the cases listed in Table I. A listing of the program and computer output is included in this section.

TABLE I  
ATTENUATION CALCULATIONS

Case	I	II	III	IV	V
Pipe ID (in)	3.75	3.75	3.75	3.75	3.75
Freq. (Hz)	6	6	24	24	24
Drilling Fluid Bulk Modulus (PSI x 10 <sup>3</sup> )	250	250	250	250	250
Mud Density (#/gal)	9	9	9	9	9
Kinematic Viscosity (cs)	10	30	10	20	30
Calculated Sound Velocity (ft/sec)	4149	4149	4149	4149	4149
Calculated "Half Depth" (ft.)	9972	5757	4986	3525	2879

Comparisons of the theory with a similar mathematical form, but incorporating experimental data are made in the following section.

```

2000 THIS PROGRAM IS BASED ON THE SECTION: "DAMPING OF SOUND IN NARROW CHANNELS"
    IN LAMBERT'S HYDRODYNAMICS, PAGES 452 AND 453
210 PRINT, "INSIDE DIAMETER OF PIPE, INCHES"
215 INPUT, DIA
216 SF=DIA/2
220 PRINT, "PRESSURE PULSE FREQUENCY, CPS"
225 INPUT, SF
230 PRINT, "BULK MODULUS OF DRILLING MUD, PSI"
235 INPUT, E
240 PRINT, "DENSITY OF DRILLING MUD, LBS/GAL"
245 INPUT, GAM
250 PRINT, "VISCOSITY OF DRILLING MUD, CENTISTOKES"
255 INPUT, XNU
260 SA=SF/12
290 E=E*144
300 RHO=GAM*7.481/32.2
320 XNU=XNU*107.74/10**7
330 OMEG=2*3.14159*SF
340 SIG=OMEG
360 SC=SQRT(E/RHO)
370 CL=SA*SC*SQRT(2/(XNU*SIG))
371 CL2=CL*ALOG(2)
400 PRINT 10, SC
410 10 FORMAT(1X, "SPEED OF SOUND IS", F8.1, 2X, "FT PER SEC")
420 PRINT 20, CL2
430 20 FORMAT(1X, "HALF PRESSURE DISTANCE IS", F8.1, 2X, "FEET")
450 PRINT 30
455 30 FORMAT(///)
460 PRINT 40
470 40 FORMAT(2X, "DISTANCE", 2X, "PRESSURE")
475 PRINT 50
480 50 FORMAT(3X, "(FEET)", 5X, "RATIO", /)
490 DL=500
500 DO 100 I=1, 21
510 XI=I-1
520 X=XI*DL
530 PR=EXP(-X/CL)
540 PRINT 110, X, PR
550 110 FORMAT(F9.0, 4X, F7.5)
560 100 CONTINUE
570 PRINT 150
575 150 FORMAT(///)
580 BETA=SQRT(SIG/(2*XNU))
610 BETA1=1/BETA
620 PRINT 200, BETA1
625 200 FORMAT(1X, "1/BETA IS", F10.7, 2X, "FT")
630 PRINT 210, SA
635 210 FORMAT(1X, "PIPE RADIUS IS", F10.5, 2X, "FT", /)
640 STOP:END

```

READY



PROGRAM  
PULSTAC  
ID:WJMTUP83  
SYSTEM- F77  
NEW OR OLD-  
OLD PULSTAC

CASE I

READY  
RUN

PULSTAC 12:410ST 03/10/80

INSIDE DIAMETER OF PIPE, INCHES73.75

PRESSURE PULSE FREQUENCY, CPS76

BULK MODULUS OF DRILLING MUD, PSI7250000

DENSITY OF DRILLING MUD, LBS/GAL79

VISCOSITY OF DRILLING MUD, CENTISTOKES710

SPEED OF SOUND IS 4149.3 FT PER SEC  
HALF PRESSURE DISTANCE IS 9972.1 FEET

DISTANCE (FEET)	PRESSURE RATIO
--------------------	-------------------

0.	1.00000
500.	0.96584
1000.	0.93285
1500.	0.90099
2000.	0.87021
2500.	0.84049
3000.	0.81178
3500.	0.78405
4000.	0.75727
4500.	0.73140
5000.	0.70642
5500.	0.68229
6000.	0.65899
6500.	0.63648
7000.	0.61474
7500.	0.59374
8000.	0.57346
8500.	0.55387
9000.	0.53495
9500.	0.51668
10000.	0.49903

1/BETA IS 0.0023908 FT  
PIPE RADIUS IS 0.15625 FT

PROGRAM STOP AT 640

RUN

PULSTAC 12:4201T 03/10/80

INSIDE DIAMETER OF PIPE, INCHES73.75

PRESSURE PULSE FREQUENCY, CPS76

CASE II

BULK MODULUS OF DRILLING MUD, PSI7250000

DENSITY OF DRILLING MUD, LBS/GAL79

VISCOSITY OF DRILLING MUD, CENTISTOKES730

SPEED OF SOUND IS 4149.3 FT PER SEC  
HALF PRESSURE DISTANCE IS 5757.4 FEET

DISTANCE (FEET)	PRESSURE RATIO
--------------------	-------------------

0.	1.00000
500.	0.94158
1000.	0.88657
1500.	0.83478
2000.	0.78601
2500.	0.74009
3000.	0.69685
3500.	0.65614
4000.	0.61781
4500.	0.58172
5000.	0.54773
5500.	0.51574
6000.	0.48561
6500.	0.45724
7000.	0.43052
7500.	0.40537
8000.	0.38169
8500.	0.35939
9000.	0.33840
9500.	0.31863
10000.	0.30001

1/BETA IS 0.0041409 FT  
PIPE RADIUS IS 0.15625 FT

PROGRAM STOP AT 10

USED 3.21 UNITS

RUN

PULSTAC 12:4303T 03/10/80

INSIDE DIAMETER OF PIPE, INCHES 33.75

PRESSURE PULSE FREQUENCY, CPS 324

CASE III

BULK MODULUS OF DRILLING MUD, PSI 250000

DENSITY OF DRILLING MUD, LBS/GAL 79

VISCOSITY OF DRILLING MUD, CENTISTOKES 710

SPEED OF SOUND IS 4149.3 FT PER SEC  
HALF PRESSURE DISTANCE IS 4996.0 FEET

DISTANCE (FEET)	PRESSURE RATIO
0.	1.00000
500.	0.93285
1000.	0.87021
1500.	0.81178
2000.	0.75727
2500.	0.70642
3000.	0.65899
3500.	0.61474
4000.	0.57346
4500.	0.53495
5000.	0.49903
5500.	0.46552
6000.	0.43426
6500.	0.40510
7000.	0.37790
7500.	0.35252
8000.	0.32885
8500.	0.30677
9000.	0.28617
9500.	0.26696
10000.	0.24903

1/BETA IS 0.0011954 FT  
PIPE RADIUS IS 0.15625 FT

PROGRAM STOP AT 640

USED 3.19 UNITS

INSIDE DIAMETER OF PIPE, INCHES 173.75

PRESSURE PULSE FREQUENCY, CPS 724

BULK MODULUS OF DRILLING MUD, PSI 250000

DENSITY OF DRILLING MUD, LBS/GAL 79

VISCOSITY OF DRILLING MUD, CENTISTOKES 720

SPEED OF SOUND IS 4149.3 FT PER SEC  
 HALF PRESSURE DISTANCE IS 3525.7 FEET

CASE IV

DISTANCE (FEET)	PRESSURE RATIO
0.	1.00000
500.	0.90638
1000.	0.82152
1500.	0.74460
2000.	0.67489
2500.	0.61171
3000.	0.55444
3500.	0.50253
4000.	0.45548
4500.	0.41284
5000.	0.37418
5500.	0.33915
6000.	0.30740
6500.	0.27862
7000.	0.25253
7500.	0.22889
8000.	0.20746
8500.	0.18804
9000.	0.17043
9500.	0.15448
10000.	0.14001

1/BETA IS 0.0016905 FT  
 PIPE RADIUS IS 0.15625 FT

PROGRAM STOP AT 640

12

USED 3.14 UNIT

PULSTAC 12:4500T 03/10/80

INSIDE DIAMETER OF PIPE, INCHES 3.75

PRESSURE PULSE FREQUENCY, CPS 24

CASE V

BULK MODULUS OF DRILLING MUD, PSI 250000

DENSITY OF DRILLING MUD, LBS/GAL 79

VISCOSITY OF DRILLING MUD, CENTISTOKES 30

SPEED OF SOUND IS 4149.3 FT PER SEC  
HALF PRESSURE DISTANCE IS 2878.7 FEET

DISTANCE (FEET)	PRESSURE RATIO
--------------------	-------------------

0.	1.00000
500.	0.88657
1000.	0.78601
1500.	0.69685
2000.	0.61781
2500.	0.54773
3000.	0.48561
3500.	0.43052
4000.	0.38169
4500.	0.33840
5000.	0.30001
5500.	0.26598
6000.	0.23581
6500.	0.20907
7000.	0.18535
7500.	0.16433
8000.	0.14569
8500.	0.12916
9000.	0.11451
9500.	0.10152
10000.	0.09001

BETA IS 0.0020705 FT  
PIPE RADIUS IS 0.15625 FT

PROGRAM STOP AT 640

LED 3.24 UNIT

## EMPIRICAL CALIBRATION OF THE THEORY

Theory indicates that the mud pulse attenuation "half depth",  $D$ , is of the form:

$$D = \text{CONSTANT} \left[ \frac{d \times c}{\sqrt{f \times v}} \right]$$

where

$d$  = effective internal pipe diameter (inches)

$c$  = speed of sound in mud (ft/sec)

$f$  = frequency (RPM)

$v$  = viscosity (cs)

$D$  = "half depth" (ft), the well depth that attenuates the mud pulse signal to one-half its original strength (2D means one-fourth remains, 3D means one-eighth, etc.)

The mathematical approach described earlier gives a theoretical value for the constant ( $K$ ) of  $K = 38.3$  with the mixed units described above. This is approximately 8.6% higher than the value of  $K = 35.3$  derived below from the data of Patton.\* This excellent match is obtained using a pipe diameter equal to the ID of the tool joint, which is the smallest diameter in the drill string. Also this is approximately the same ID as the collars.

---

\* Patton et al, "Development and Successful Testing of a Continuous Wave," Logging-While-Drilling Telemetry System, J. Pet. Tech., Oct. 1977.

From this point forward, the empirical calibration of the theory will be used.

Calibrating against the data of Patton:

$$D = 10^4 \text{ ft}$$

$$d = 2.5 \text{ in}$$

$$c = 4300 \text{ ft/sec}$$

$$f = 24 \frac{\text{cyc}}{\text{sec}} \left( 60 \frac{\text{sec}}{\text{min}} \right) = 1440 \text{ RPM}$$

$$v = 1 \text{ cs}$$

$$\text{CONSTANT} = K$$

$$= D \times \frac{\sqrt{f \times v}}{d \times c}$$

$$= 10^4 \times \frac{\sqrt{1440}}{2 \times 5(4300)}$$

$$K = 35.3$$

$$D = 35.3 \frac{d \times c}{\sqrt{f \times v}}$$

Lack of knowledge of the kinematic viscosity is a basic limitation to using the calculation in oil field and geothermal situations. As a first approximation, we may assume that the Bingham Plastic Viscosity (PV) of the drilling fluid is a good estimate of the absolute viscosity. To obtain kinematic viscosity, the absolute viscosity is scaled by fluid density. In oil field units

$$v(\text{cs}) = \text{PV}(\text{cp}) \frac{8.34}{\text{Mud Wt. (PPG)}}$$

TABLE II

CALCULATION OF HALF-DEPTH FOR THE  
EXPECTED RANGE OF VARIABLES

	<u>Maximum Range</u>		<u>Typical Range</u>	
	Low	High	Low	High
d(inch)	5	2	4	2.5
c(ft/sec)	5000	4000	4500	4300
f(RPM)	3000	1	1200	20
v(cs)	50	1	20	5
D(1000 ft)	2.3	282.4	4.1	37.9



## NOMOGRAM SOLUTION TO THE ATTENUATION CALCULATION

The calculation of attenuation "Half Depth" can be usefully expressed in nomogram form. The nomogram is derived and presented in this chapter.

### Nomogram Calculation

$$D = 35.3 \frac{d \times c}{\sqrt{f \times v}}$$

let  $d = 3$ ,  $c = 4500$

$$D(1000 \text{ ft}) = \left(\frac{476.6}{\sqrt{v}}\right) \times \left(\frac{1}{\sqrt{f}}\right)$$

Half Depth (1,000 ft)

Freq. (RPM)	$v = 1$ $D =$ 476.6 $\left(\frac{1}{\sqrt{f}}\right)$	$v = 1$ $D =$ 276.1 $\left(\frac{1}{\sqrt{f}}\right)$	$v = 1$ $D =$ 150.7 $\left(\frac{1}{\sqrt{f}}\right)$	$v = 1$ $D =$ 87.0 $\left(\frac{1}{\sqrt{f}}\right)$	$v = 1$ $D =$ 47.7 $\left(\frac{1}{\sqrt{f}}\right)$
1	476.6	275.1	150.7	87.0	47.7
10	150.7	87.0	47.7	27.5	15.1
100	47.7	27.5	15.1	8.70	4.77
1,000	15.1	8.70	4.77	2.75	1.51
10,000	4.77	2.75	1.51	0.87	.48